4.2 Fuel System Design

The fuel system is designed to satisfy the following criteria:

- The fuel system will not be damaged as a result of normal operation and anticipated operational occurrences (AOO) (GDC 10).
- Fuel damage during postulated accidents (PA) will not be severe enough to prevent control rod insertion when it is required (GDC 27).
- Core coolability will always be maintained, even after severe PAs (GDC 35 and 10 CFR 50.34).
- The number of fuel rod failures is not underestimated for PAs. The response of the fuel system design to PAs is presented in Chapter 15 (10 CFR 50.46).

The general design features of U.S. EPR fuel assemblies include the following:

- 17x17 lattice design.
- Lattice includes 24 guide tube locations and 265 fuel rods.
- Center instrument tube cell location replaced by a fuel rod.
- Removable top nozzle optimized for low pressure drop with quarter-turn quick-disconnect feature.
- Nominal fuel length is approximately 13.8 ft.
- Incore detectors are top loaded and occupy selected guide tube locations.
- Alloy M5™ fuel rod cladding.
- M5™ MONOBLOC™ guide tubes.
- Alloy 718, high mechanical performance (HMP) upper and lower end grids.
- Eight M5™ high thermal performance (HTP) intermediate grids.
- Robust FUELGUARD™ bottom nozzle.
- 62 GWD/MTU fuel rod burnup limit.
- Selected fuel assemblies have burnable poison rods with up to eight weight percent Gd_2O_3 (from four to 28 rods per assembly).
- No separate burnable poison rod assemblies.
- Axial blankets to reduce axial neutron leakage and improve fuel economy.

- Design power histories that are based on 18 and 24 month fuel cycles.
- Varying radial and axial fuel enrichments to control power peaking.
- Accommodates 0.3 g safe shutdown earthquake (SSE) spectra.
- Quick-disconnect (QD) top nozzle uses a leaf spring hold-down system and a low pressure drop nozzle structure.
- A welded cage design to improve fuel assembly bow performance.

4.2.1 Design Bases

The fuel assembly and fuel rod design bases are defined in U.S. EPR Fuel Assembly Mechanical Design (Reference 1) and are summarized in this section.

4.2.1.1 Cladding

The fuel rod cladding is M5™ material that has been approved for use in Evaluation of Advanced Cladding and Structural Material (M5™) in PWR Reactor Fuel (Reference 2). The major dimensions of the cladding are shown in Table 4.2-1—U.S. EPR Fuel Assembly Design Summary. Dimensions and other cladding information are provided in Reference 1 and summarized later in this section.

4.2.1.1.1 Mechanical Properties of Cladding

The fuel rod cladding properties are defined in "Evaluation of Advanced Cladding and Structural Material (M5™) in PWR Reactor Fuel," (Reference 2) and justified for use in the Codes and Methods Applicability Report for the U.S. EPR (Reference 3).

4.2.1.1.2 Stress-Strain Limits of Cladding

Reference 2 provides the methodology and design criteria for analyzing cladding stress. The cladding stress analysis follows the guidelines of Division 1, Subsection NG of the ASME Boiler and Pressure Vessel Code, Section III (Reference 4), which specifies the use of stress intensities (a method known as the maximum shear stress criteria). The stress states modeled for the M5™ cladding are maximum compression and maximum tension. As approved in Reference 2, the primary membrane stress intensity limit is 1.5 Sm for the compression case and 1.0 Sm for the tension case. In all other cases, the stress intensity limits are the same as those defined in the ASME Code.

To determine the stress limits for M5™ cladding applications, the design criteria for fuel rod cladding stresses are based on unirradiated yield and ultimate tensile strengths, as approved in Reference 2. The use of unirradiated values is conservative

because irradiation increases the yield and ultimate tensile strengths for M5™ and other zirconium alloys.

The stress analysis of the fuel rod design accounts for the following sources of cladding stress:

- Pressure differentials.
- Ovality.
- Thermal differentials.
- Flow induced vibration (FIV).
- Fuel rod growth.
- Fuel rod and spacer grid interaction.
- Plenum spring force.

A cladding buckling analysis determined that when the rod internal pressure is at a minimum and the system pressure is at a maximum, the cladding does not buckle. The method and equations used for the buckling analysis are presented in Reference 2.

For cladding strain, the maximum uniform hoop strain (elastic plus plastic) in the cladding does not exceed one percent, which precludes excessive cladding deformation from normal operation and AOOs. This cladding strain criterion has been approved in Reference 2.

4.2.1.1.3 Vibration and Fatigue of Cladding

The cumulative fatigue usage factor does not exceed 1.0. The analysis method is consistent with the procedure for fatigue analysis provided in Subparagraph NG-3222.4 of the ASME Code (Reference 4). To provide a conservative design, the design fatigue curve applies a safety factor of two on stress amplitude or a factor of 20 on the number of cycles, whichever is most conservative at each point.

The design criterion against fretting wear is that the fuel design provides the necessary support to limit fuel rod vibration and cladding fretting wear. This criterion has been approved in Reference 2 and found to be acceptable for the fuel rod design up to the burnup limit of 62 GWD/MTU as established in Extended Burnup Evaluation (Reference 5).

4.2.1.1.4 Chemical Properties of Cladding

The predicted external cladding oxide thickness is well below the maximum oxide thickness limit established for the U.S. EPR in Reference 5.

Controlling the level of hydrogen impurities in the fuel during fabrication precludes internal hydriding as a cladding failure mechanism.

Maintaining the oxide thickness below the maximum limit specified in Reference 5 precludes external hydriding as a cladding failure mechanism.

4.2.1.2 Fuel Material

4.2.1.2.1 Thermal-Physical Properties of Fuel Material

The thermal-physical properties of the fuel are presented in the COPERNIC Fuel Rod Design Computer Code (Reference 6).

4.2.1.2.2 Fuel Densification and Fission Product Swelling

Fuel densification and fission product swelling are addressed in Reference 6.

4.2.1.2.3 Chemical Properties of Fuel Material

The chemical properties of the fuel are tightly controlled to minimize pellet interactions with the cladding, to minimize the introduction of contaminants into the fuel rods, and to maintain pellet performance within code predictions. Chemical properties are controlled through a rigorous testing and inspection program to demonstrate that each lot of pellets conforms to design requirements and criteria (see Section 4.2.3.2.2).

4.2.1.3 Fuel Rod Performance

4.2.1.3.1 Analytical Models

The computer code COPERNIC (Reference 6) is used to perform the thermal-mechanical analyses to simulate the behavior of the fuel rod during irradiation, and is also used to verify that the U.S. EPR fuel rod design meets design and safety criteria. The critical design bases addressed with COPERNIC include fuel rod internal pressures, cladding temperatures, cladding strain, corrosion, and centerline fuel melt under conditions of normal operation, AOOs, and PAs. Reference 1 provides additional details concerning the design basis for normal operations and AOOs. Section 4.4 addresses DNB design criteria. Section 15.4 covers reactivity initiated accidents, insertion accidents, and pellet temperatures. Creep collapse is analyzed with the methods and codes described in Reference 2. The applicability of References 2 and 6 to the U.S. EPR is justified in the Codes and Methods Topical Report (Reference 3).

4.2.1.3.2 Models Predictions

The predicted collapse life of the fuel rod exceeds the maximum expected incore life. Stable fuel designs have minimized densification, which otherwise can cause gaps in

the fuel column into which the cladding could ovalize and collapse. The U.S. EPR fuel pellets have an as-fabricated density of 96 percent of the theoretical density (TD) and exhibit very low densification (the upper tolerance limit is 1.5 percent TD). In addition, online inspections during the fuel rod manufacturing process guard against fuel column gaps occurring before the rod is placed in the reactor. These factors create a fuel column that is unlikely to develop gaps during its lifetime, precluding the possibility of creep collapse.

The fuel rod internal pressure criteria are defined in Reference 2 and in Fuel Rod Gas Pressure Criterion (Reference 7). The design basis is that the fuel system will not be damaged due to excessive fuel rod internal pressure. The internal pressure of the peak power fuel rod in the reactor is maintained below a value that would cause the fuel-to-cladding gap to increase because of cladding outward creep during steady-state operation, and extensive departure from nucleate boiling (DNB) propagation to occur. In no case during normal operation will the internal pressure of the peak power rod exceed the reactor coolant system (RCS) pressure by more than the value presented in Reference 7.

4.2.1.3.3 Analytical Models Uncertainties

The analytical uncertainties used in the COPERNIC fuel rod models are addressed in Reference 6.

4.2.1.4 HMP End Grids and HTP Intermediate Grids

The end spacer grids (top and bottom) are made of Alloy 718 and are the AREVA NP HMP design. The intermediate spacer grids (eight per fuel assembly) are M5™ strip material and are the AREVA NP HTP design. The grids provide lateral and rotational end fixity for guide tube buckling resistance and provide restraint for the fuel rods. The major parameters of the HMP end spacer grid and the HTP intermediate spacer girds are provided in Reference 1.

The spacer grids are designed to maintain the fuel rods in a coolable configuration (GDC 35 and 10 CFR 50.34), and allow for control rod insertion for AOOs and PAs (GDC 27). Structural evaluations of the grids determined that for all cases the resulting impact loads are lower than the tested loads at which deformations occur. The evaluation methodology used is consistent with the loss-of-coolant accident (LOCA) and seismic analyses methodology approved in Mark-C Fuel Assembly LOCA-Seismic Analyses (Reference 8). This methodology uses the load limits that are derived by testing, which are provided in Reference 1 for the fuel assembly mechanical design.

4.2.1.4.1 Mechanical, Chemical, Thermal, and Irradiation Properties of Grids

Mechanical, chemical, thermal, and irradiation properties of the M5™ used for the HTP spacer grid and guide tubes are presented in Reference 2.

The strength criteria of the fuel assembly 17x17 grid components are based on mechanical strength testing of prototypes, including static and dynamic crush testing. The design limits are detailed in the U.S. EPR Fuel Assembly Mechanical Design Topical Report (Reference 1). The grids were tested to a 95 percent confidence level of the mean elastic impact load limit for beginning of life (BOL) at operating temperature. The design limit derived from this test is provided in Reference 1. This limit is sufficient to demonstrate that, under worst-case combined seismic and LOCA events, the core, from a grid perspective, will remain in a coolable geometry (GDC 35 and 10 CFR 50.34).

The evaluation methods used for evaluation of faulted conditions have been approved in Reference 8. This methodology will be applicable to the U.S. EPR fuel assembly design upon approval of Reference 1.

The allowable grid clamping loads during fuel shipment are based on static crush strength testing for static stiffness and elastic load limits. The spacer grids maintain their structural integrity under the maximum lateral shipping loads and the maximum clamping loads. The spacer grid springs are designed to maintain acceptable fuel rod grip forces from the 6g lateral and 4g axial shipping loads.

Spacer grid slip load input to the analytical models of the fuel assembly used in the horizontal and vertical faulted analyses are established by mechanical testing.

4.2.1.4.2 Vibration and Fatigue of Grids

Interference between spacer grids and fuel rods is maintained throughout the life of the fuel assembly, so fuel rod cladding wear is expected to be well below acceptable limits (see Section 4.2.1.1.3). The interface between the fuel rods and the spacer grids will prevent fuel rod fretting failure.

4.2.1.4.3 Chemical Compatibility of Grids with other Core Components

The M5™ materials of the spacer grids are compatible with the reactor coolant. Properties of the M5™ spacer grid and guide tube material are provided in Reference 2.

The compatibility of M5™ materials with other core components, such as stainless steels, has been verified by both operating experience and in the evaluation provided in Reference 2.

4.2.1.5 Fuel Assembly Structural and Thermal-Hydraulic Design

The fuel assemblies accept control rod insertions to provide the reactivity control for power operations and reactor shutdown. The structural integrity of the fuel

assemblies is maintained by setting design limits on stresses and deformations from various nonoperational, normal operational, AOO, and PA loads, including:

- Nonoperational: 4g axial and 6g lateral loading with dimensional stability.
- Normal operating, AOOs, and PAs: The fuel assembly component structural design criteria are established for the two primary material categories, austenitic stainless steels and M5™. The stress categories and strength theory presented in ASME Code, Section III, Subsection NG (Reference 4) are used as a guide. In general, components are designed by analysis to the maximum shear-theory (Tresca criterion) for combined stresses. The stress intensity is defined as the numerically largest difference between the various principal stresses in a three-dimensional field. In other cases, strain energy theory (Von-Mises criterion) for the combined stresses in the principal directions is used.

The thermal-hydraulic design basis for the U.S. EPR fuel assembly is presented in Section 4.4 and Reference 1.

4.2.1.5.1 Nonoperational Loading

The nonoperational loading, with dimensional stability, is 4g axial and 6g lateral.

4.2.1.5.2 Normal Operational Conditions and Anticipated Operational Occurrences

For normal operating conditions, the allowable stress intensity (Sm) values for austenitic steels, such as nickel-chromium-iron alloys, is given by the lower of the following:

- One-third of the specified minimum tensile strength (Su) or two-thirds of the specified minimum yield strength (Sy) at room temperature.
- One-third of the tensile strength or 90 percent of the yield strength at temperature, but not to exceed two-thirds of the specified minimum yield strength at room temperature.

The stress limits for normal operating conditions for the austenitic steel components are as follows:

- General primary membrane stress intensity limit is Sm.
- Primary membrane plus bending stress intensity limit is 1.5 Sm.
- Total primary plus secondary stress intensity limit is 3.0 Sm.

The M5™ structural components, which consist of guide tube and fuel rod cladding, are divided into two categories because of material differences and functional requirements:

- The fuel rod cladding design criteria are addressed in Section 4.2.1.1.
- The maximum shear theory is used to evaluate the guide tube design. For conservative purposes, the M5™ unirradiated properties are used to define the stress limits.

4.2.1.5.3 Postulated Accident Conditions

Worst-case abnormal loads during PAs are represented by combined seismic and LOCA loads. For these conditions, the deflections or failures of components cannot interfere with the reactor shutdown or emergency cooling of the fuel rods (GDC 27, GDC 35, and 10 CFR 50.34).

The fuel assembly structural component stresses under faulted conditions are evaluated using primarily the methods outlined in Appendix F of ASME Code, Section III (Reference 4). For austenitic steel fuel assembly components, the stress intensity is defined per the rules described above for normal operating conditions. The faulted condition stress limits for fuel assembly structural components are:

- General primary membrane stress intensity limit is the smaller of 2.4 Sm or 0.70 Su.
- Primary membrane plus bending stress intensity limit is the smaller of 3.6 Sm or 1.05 Su.

For M5™ components, the stress intensity limits are set at 2/3 of the material yield strength, Sy, at reactor operating temperature:

- The stress intensity limit for the general primary membrane is the smaller of 1.6 Sy or 0.70 Su.
- The stress intensity limit for the primary membrane plus bending is the smaller of 2.4 Sy or 1.05 Su.

4.2.1.5.4 Growth Allowance

A fuel assembly nozzle-to-fuel rod shoulder gap allowance is provided to maintain positive clearance between the fuel rods and the nozzles during the entire fuel assembly lifetime.

A fuel assembly-to-reactor internals gap allowance is provided to maintain a positive core plate gap during the entire fuel assembly lifetime.

4.2.1.5.5 Hold-down Springs

The hold-down springs are capable of maintaining the fuel assembly in contact with the lower core plate during AOOs, except for pump overspeed transients. During a pump overspeed transient, the hold-down spring function is not impaired nor does the

fuel assembly top nozzle contact the upper core plate. The fuel assembly top and bottom nozzles are designed to maintain engagement with the reactor internals for AOOs and PAs. The fuel assembly design does not permit the hold-down springs to be compressed to solid height for any AOO.

4.2.1.5.6 Guide Tube Buckling

U.S. EPR guide tube evaluations demonstrate that buckling will not occur. In addition, the primary and primary-plus-secondary stresses are confirmed to be lower than the material allowable stresses in the ASME Code (Reference 4).

4.2.1.5.7 Interface with Adjacent Assemblies

To establish axial alignment of spacer grids with adjacent fuel assemblies, the HTP grids are spot welded to the guide tubes. Sleeves of M5™ are spot welded to the guide tubes above and below the HMP grids for axial location and restraint. The height of the grids is greater than the worst-case differences in grid elevation at BOL and end of life (EOL). Therefore, grid overlap between adjacent assemblies is maintained for the life of the fuel assembly. Those differences arise due to irradiation-induced length changes of the guide tubes.

4.2.1.5.8 Fuel Rod Fretting and Wear

The fuel assembly is designed to provide the support needed to limit fuel rod vibration and fretting wear. To further reduce the potential for fretting and wear, the fuel assembly is also designed to limit span-average cross flow velocities to less than 2 ft/s. (A span equals a single axial region between adjacent grids or nozzles.)

4.2.1.5.9 Fuel Rod Bow

Fuel rod bowing is evaluated with respect to the mechanical and thermal-hydraulic performance of the fuel assembly. The fuel assembly design precludes excessive bow during its operational lifetime.

4.2.1.5.10 Control Rod Trip Times

The fuel assembly will not experience any permanent deformations during AOOs that would cause the control component drop time to increase beyond the drop time criteria provided in Reference 1. This criterion is met by demonstrating the fuel assembly guide tubes remain elastic under all operating conditions.

4.2.1.5.11 Mechanical Compatibility

As the fuel assembly design evolves, any design changes will be dimensionally and hydraulically compatible with existing resident fuel within the reactor, with other core components, and with the fuel handling equipment.

4.2.1.5.12 LOCA and Seismic Loading

The fuel assembly is designed to provide safe operation following an operating basis earthquake (OBE), a safe shutdown earthquake (SSE), and a LOCA by maintaining the dimensions needed for control rod insertion and a coolable geometry. The fuel assembly supports and maintains the fuel rods in a coolable configuration for all operating conditions, including AOOs and PAs (GDC 35 and 10 CFR 50.34).

4.2.1.5.13 Shipping and Handling Loads

The fuel assembly is designed for the maximum axial pull and axial push loads occurring during handling, as presented in the Fuel Assembly Mechanical Design Topical Report (Reference 1). The fuel rods will not slip through the spacer grids under the maximum axial shipping loads.

4.2.1.5.14 Material Compatibility

Table 4.2-2—Fuel Assembly Materials, provides a list of fuel assembly components and their materials. The selection of fuel assembly materials is based on extensive operating experience and their compatibility with the service environment and with each other. Each material has been optimized for resistance to adverse changes in material properties from irradiation and has been evaluated for strength and mechanical properties for the operating temperatures and for the full service life anticipated for each component.

Each material is based on an industry standard and may be modified according to specific engineering requirements, such as lowering the cobalt content in stainless steel and nickel-based alloy components, without changing their material performance, in order to reduce activation levels.

4.2.1.5.15 Corrosion

The fuel assembly structural design evaluation considers the effects of thinning from corrosion and the effects of oxide layer formation. M5™ guide tube material corrosion allowance limits are established from operating experience, design verification testing, and similarities with existing designs. The corrosion allowance limits for M5™ components are presented in Reference 2.

The excellent corrosion resistance of the alloys used in the U.S. EPR fuel assembly has been demonstrated by extensive operating experience. This corrosion resistance is the result of both material selection and sound manufacturing techniques. Rigorous material standards provide high quality base material, while controlled manufacturing procedures produce components with a minimum of surface contamination. Manufacturing, handling, and assembly procedures prevent contaminants from

coming into contact with the metals during fabrication, welding, or annealing operations.

The low carbon in the 304L stainless steels used in the U.S. EPR provides excellent resistance to intergranular corrosion and sensitization of the metal. The activity levels caused by neutron activation of non-fuel components in the reactor is minimized by reducing the level of cobalt in the 304L stainless steel and Alloy 718 components used in the fuel assemblies.

Section 5.2.3.2 provides information on those aspects of the reactor coolant chemistry that provides corrosion protection for stainless steels and nickel alloys. A comprehensive review of the U.S. EPR reactor coolant environment and the potential effect on corrosion of these materials has been made.

4.2.1.6 Rod Cluster Control and Neutron Source Assemblies

The general design bases which have been evaluated and considered in the design and analysis for the rod cluster control assemblies (RCCA) include the following:

- 15 year minimum design lifetime.
- Nuclear reactivity control.
- Minimum and maximum reactor trip times.
- Insertability.
- Mechanical strength at ambient and elevated temperatures.
- Chemical compatibility between the control component materials.
- Chemical compatibility of the control component materials and the reactor coolant.
- Resistance to radiation degradation.

To prevent mechanical damage and to maintain the design configuration to allow RCCA insertion into the fuel assembly, the RCCAs are designed for the following operating factors:

- Differential pressure across the cladding wall.
- Temperature effects, including differential thermal expansion, thermal gradients, thermal creep, and prevention of absorber melting under normal operations and AOOs.
- Deceleration loads caused by a reactor trip.

- Control rod drive mechanism (CRDM) stepping loads during reactor operation.
- Flow induced vibrations and the resulting fatigue loads.
- Misalignment within the fuel assembly and stuck rods within the fuel assembly guide tubes.
- Irradiation effects on materials.
- Compatibility of materials with the reactor coolant system and with interfacing components.

The general design bases which have been evaluated and considered in the design and analysis for the neutron sources and thimble plug assemblies (TPA) include the following:

- Mechanical strength at ambient and elevated temperatures.
- Chemical compatibility between the control component materials.
- Chemical compatibility of the control component materials and the reactor coolant.
- Resistance to radiation degradation.

To preclude damage or loss of neutron source materials to the RCS, the neutron sources and TPAs are designed for the following reactor operating factors:

- Differential pressure across the cladding wall of the neutron source rods.
- Thermal effects (differential thermal expansion and neutron source material melting temperatures).
- Irradiation effects on materials.
- Hydraulic loading conditions.
- Hold-down of stationary control component assemblies (SCCA) spiders.
- Guidance of incore instrumentation (TPAs only).

4.2.1.6.1 Thermal-Physical Properties

The RCCA rod absorber material is a standard Ag-In-Cd (AIC) alloy of nominal composition 80 weight percent silver, 15 weight percent indium, and 5 weight percent cadmium, a composition which has been used in U.S. PWRs for many years. Current experience in the PWR reactor environment for this alloy continues to demonstrate it is compatible with the radiation, thermal, and chemical environments in which it operates.

Design bases that have been addressed for the absorber material include irradiation swelling to guard against excessive cladding stress and strain. Thermal effects have been addressed, which include absorber thermal expansion and thermal creep, both of which can contribute to absorber-cladding mechanical interaction.

Based on the relatively low melting temperature of AIC, maximum temperatures during normal operation and postulated accident conditions have been determined. The thermal response during accident conditions has been addressed because of the potential for material redistribution of the annular absorber and the associated effect on reactivity.

4.2.1.6.2 Compatibility of the Absorber and Cladding Materials

Chemical compatibility of the AIC absorber material with the cladding has been demonstrated by past reactor operating experience in PWRs. Compatibility between the two materials under accident conditions, for which the absorber is postulated to melt, has also been evaluated.

Chemical compatibility between control component materials that are exposed to reactor coolant has been evaluated and addressed. Again, acceptability is based largely on past reactor operating experience with the materials comprising the U.S. EPR RCCA (including, austenitic stainless steels, AIC, and nickel Alloy 718). Section 5.2.3 provides further details on compatibility of these materials with the reactor coolant.

4.2.1.6.3 Stress-Strain Limits

For normal operations and AOOs, the stress limits used are consistent with Subsection NG of the ASME Code, Section III (Reference 4) for the structural members of the control components, including RCCA rod cladding. The maximum shear stress theory stipulated by the code is used in the analysis for the cladding and spider structural response. Fatigue limits are also based on ASME Code criteria.

Circumferential cladding stresses may develop slowly from the mechanical interaction between the cladding and AIC absorber, which swells from radiation exposure at the lower tip region. Cladding stress limits from this time-dependent AIC swelling are based on conservative cladding fracture limits.

4.2.1.6.4 Irradiation Behavior of Absorber Material

The following irradiation effects have been considered in the analysis for the control components:

- Irradiation swelling of the AIC absorber material.
- Irradiation swelling of the alumina spacers within the primary neutron source assembly.

- Internal gas generation resulting from neutron capture by the antimony-beryllium secondary neutron source material.
- Maximum temperatures attained by the AIC absorber under normal operating conditions, AOOs, and PAs.
- Maximum temperatures for the Cf-252 primary source material under normal operation and AOOs.

4.2.1.7 Surveillance Programs

The fuel system surveillance program subjects fuel rods and fuel assemblies to post-irradiation examinations that generally include measuring cladding oxide thickness, rod diameter, rod length growth, bowing, shoulder gap, and overall fuel assembly growth. The overall fuel rod and assembly conditions are also visually examined during postirradiation examinations for indications of mechanical damage.

The RCCA surveillance program serves as a means of monitoring control rod integrity. Inspections are performed to determine the presence and extent of cladding wear from interactions with reactor vessel internals and fuel assembly guide tubes. The ion-nitrided hardened outer surface provides for improved wear resistance over non-treated stainless steel tubing surfaces. However, some level of wear is still expected and the extent of cladding wear should be monitored. Verification of the cladding integrity also includes monitoring for the absence of excessive cladding strain and potential cracking from AIC absorber swelling.

4.2.2 Description and Design Drawings

The details of the fuel assembly design description and design drawings are in the Fuel Assembly Mechanical Design Topical Report (Reference 1).

4.2.2.1 Fuel Assembly Description

The U.S. EPR fuel assembly is a 17x17 array of fuel rods that have been designed specifically for use with the core configuration of the U.S. EPR reactor. The main fuel assembly parameters are listed in Table 4.2-1 and the fuel assembly and fuel rods are illustrated in Figure 4.2-1—U.S. EPR Fuel Assembly, and Figure 4.2-2—Fuel Rod Assembly, respectively. This design does not require a central instrument tube in the assembly, as instrumentation lances are inserted into a small subset of guide tube locations (See Figure 4.2-3—Instrument Lance Position).

The fuel assembly uses 10 spacer grids that, with the 24 guide tubes and a top and a bottom nozzle, provide the structural cage (skeleton) for supporting the 265 fuel rods. The top and bottom grids are constructed of Alloy 718 strip material and use the AREVA NP HMP design, while the eight intermediate HTP grids are constructed from

M5™ strip material. The M5™ clad fuel rods are laterally supported by the top and bottom HMP end spacer grids and the eight HTP intermediate spacer grids.

Features on the guide tube assemblies constrain axial motion of the end grids. Both top and bottom HMP end grids are axially restrained by short M5™ spacer sleeves welded directly to the guide tube above and below each grid.

The fuel assembly is designed for a normal operating coolant pressure of 2250 psia, and a maximum fuel rod burnup of 62 GWD/MTU.

Each fuel assembly can operate in any core location. Proper orientation of the fuel assembly in the core is established by a hole in one corner of the top nozzle which prevents improper interface with the refueling machine via a mating pin on the refueling machine grapple. The refueling machine then provides the proper orientation of the fuel assembly in storage, during refueling transport, and in the reactor core operating position.

4.2.2.2 Spacer Grids Description

The fuel assembly uses HTP spacer grids at the intermediate locations and HMP spacer grids at the top and bottom locations of the assembly. Some key grid parameters are presented in Reference 1 and summarized below. The HTP grids are constructed of M5™ alloy strip for enhanced corrosion resistance and low irradiation growth. The HMP grids are constructed of Alloy 718 strip for enhanced strength and low cell relaxation during irradiation. The use of the M5™ alloy for spacer grids is addressed in Reference 2. In addition, the alloy is applicable for the U.S. EPR fuel design per the Codes and Methods Topical Report (Reference 3).

Each HTP grid is an M5™ structure of interlocking strips that are welded together at each strip intersection to form a 17 x 17 matrix of square cells. Each cross-strip is formed by resistance spot welding two stamped M5™ halves to form a doublet. The assembled doublets contain channels, slanted at the outlets, which induce a swirling pattern in the coolant flow, as illustrated in Figure 4.2-4—Intermediate HTP Spacer Grid Cross-Section, and Figure 4.2-5—HTP Spacer Grid Characteristics. The channels are arranged so that there is no net torque on the fuel assembly. These channels also provide the contact surfaces that hold the fuel rods in place. The channel strips are formed in the axial direction so that they provide a spring contact with the fuel rods in the mid-region of the spacer. At the inlet and outlet of the spacer, the channels, referred to as castellations, provide more rigid lateral constraint at a slight nominal clearance from the fuel rod. Sideplates are welded to the ends of the doublets. The sideplates are provided with top and bottom lead-in tabs so as to avoid assembly hang-up during fuel movement.

HMP grids (see Figure 4.2-6—HMP End Grid Assembly) are constructed of low cobalt, precipitation-hardened Alloy 718 strip material. Resilient spring features are stamped into the strips that provide frictional axial restraint of each interfacing fuel rod by an interference fit of the fuel rods within each grid cell. Spring and friction contact with each fuel rod is maintained throughout the life of the fuel assembly up to the design burnup. Each HMP spacer grid maintains eight individual line contacts per cell with each fuel rod (similar to the HTP spacer) and relaxation of the spring within each cell due to irradiation is minimized by the low relaxation properties of Alloy 718 material. Since HMP grid cell relaxation is minimal, the fuel rod position is maintained during the life of the fuel assembly. HMP spacer grids are similar to HTP spacer grids, except for the material of construction and the fact that the flow channels created by the doublets are straight, and do not produce swirling flow around the fuel rods.

To maintain axial alignment of spacer grids with adjacent fuel assemblies, all of the HTP grids are spot welded to the guide tubes. This limits grid axial movement after irradiation relaxation. Short M5™ sleeves are spot welded to the guide tube at locations above and below each HMP grid.

4.2.2.3 Quick Disconnect Mechanism Description

A quick disconnect (QD) mechanism attaches the top nozzle to the guide tubes (see Figure 4.2-7—Guide Tube QD Connection with Top Nozzle, and Figure 4.2-8—MONOBLOC™ Guide Tube Assembly. This interface design allows the top nozzle to be removed for fuel assembly reconstitution. The design consists of a double-spline sleeve made of M5™ alloy attached to the guide tube via multiple spot welds. Machined keyway-type features within the interfacing guide tube attachment holes in the top nozzle provide either clearance for removal or restraint for securing the nozzle, based on the clock orientation of QD features on the guide tube assemblies. The reconstitution tooling rotates the guide tube QD ring 90° to lock or unlock the guide tube connection, and provides a rigid connection when the ring is rotated to its locking position.

4.2.2.4 Top Nozzle Assembly Description

The top nozzle structure (see Figure 4.2-9—QD Top Nozzle Assembly) consists of a stainless steel frame that interfaces with the reactor upper internals and the core components while providing for coolant flow. The top nozzle flow-hole pattern provides an increased flow area, yielding a low pressure-drop while satisfying strength requirements. The low pressure-drop feature is achieved by optimizing the flow path geometry with the nozzle structural integrity that accommodates each required normal and faulted load. The top nozzle design also incorporates a QD feature to attach to the 24 fuel assembly guide tubes, as presented in Section 4.2.2.3. The primary features of the top nozzle include:

- Five leaf spring hold-down system (Section 4.2.2.5).
- Low pressure-drop nozzle structure.
- QD guide tube attachment (Section 4.2.2.3).

4.2.2.5 Hold-down Springs Description

The leaf spring design consists of four sets of five leaf springs made of Alloy 718 (see Figure 4.2-9). Located in the top nozzle, the spring maintains positive fuel assembly contact with the core support structure under normal operating conditions and also maintains a positive hold-down margin for the flow forces. The leaf spring sets are fastened to the top nozzle with Alloy 718 clamp screws. The upper leaf has an extended tang that engages a cutout in the top plate of the nozzle. This arrangement maintains spring leaf retention in the unlikely event of a single spring leaf or clamp screw failure.

4.2.2.6 Bottom Nozzle Description

The U.S. EPR fuel assembly uses the FUELGUARD™ debris resistant bottom nozzle (see Figure 4.2-10—FUELGUARD™ Lower Nozzle Arrangement). It is constructed of stainless steel, has a frame of deep ribs connecting the guide tube attachment bushings, and has conventional legs that interface with the reactor internals. The frame distributes the primary loads on the fuel assembly through the bottom nozzle. A set of curved blades are brazed into the frame structure which provide good flow characteristics and enhanced debris filtering. The guide tube lower end plugs are threaded to rigidly connect the guide tubes to the bottom nozzle with special screws. The FUELGUARD™ lower tie plate provides an effective barrier to debris.

A guide tube connection with the bottom nozzle is shown in Figure 4.2-11—Guide Tube Screw Connection at Bottom Nozzle.

4.2.2.7 MONOBLOC™ Guide Tubes Description

MONOBLOC™ guide tubes are fabricated from M5™ alloy. The use of M5™ alloy for guide tubes is approved in References 2 and 3, and in Incorporation of M5™ Properties in Framatome ANP Approved Methods (Reference 9). This material exhibits low corrosion and low hydrogen uptake throughout the fuel design burnup range and low irradiation growth rates.

Each MONOBLOC™ guide tube, as shown in Figure 4.2-8, has two inside diameters (ID) and a single outside diameter (OD). The larger ID at the top provides a relatively large annular clearance that permits rapid insertion of the RCCA during a reactor trip and also accommodates coolant flow during normal operation with inserted control rods. The reduced ID section (i.e., the dashpot located at the bottom end of the tube)

provides a close fit with the control rods to facilitate deceleration toward the end of the control rod travel. This deceleration limits the magnitude of the RCCA impact loads on the fuel assembly top nozzle. The guide tube wall thickness at the bottom is much greater in the dashpot region than at the upper end to maintain the same OD with the smaller dashpot ID. The MONOBLOC™ design provides a rigid tube and robust guide tube structure that helps to minimize fuel assembly distortion and bow.

Four small holes in the guide tube located just above the dashpot allow both outflow of water during RCCA insertion, and coolant bypass flow to the control components and instrumentation lances during operation. There is also a small flow hole in the guide tube bolt that enables some coolant flow through the reduced diameter section and drainage of the guide tube, as well as displaced coolant venting during RCCA deceleration.

The QD sleeve is attached to the upper end of the guide tube and connects to the top nozzle. The guide tube connection between the guide tube end plug and the bottom nozzle is illustrated in Figure 4.2-11. A 316L stainless steel fastener threads into a threaded M5™ end plug that is welded to the end of each guide tube. The 304L stainless steel bottom nozzle is captured and compressed by the fastener to form the joint.

4.2.2.8 Fuel Rods Description

The U.S. EPR fuel rod design consists of uranium dioxide (UO_2) pellets contained in a seamless M5™ zirconium alloy tube, with M5™ end plugs welded at each end. The use of M5™ material is approved in References 2 and 9. Compared to earlier zirconium alloys, M5™ cladding significantly increases the resistance to corrosion associated with longer fuel cycles, higher operating temperatures, and higher burnup. The fuel rod length and void volume provide acceptable margin against failure by internal pressure buildup. The fuel rod uses one stainless steel spring in the upper plenum to prevent the formation of fuel pellet stack gaps during shipping and handling, while also allowing for the expansion of the fuel stack during operation. The fuel stack rests on a lower support tube, which in turn sits on the lower end plug. This lower support tube provides additional plenum volume in the fuel rod. The M5™ upper and lower end plugs are identical. The shape of the end plug allows the fuel rods to be gripped so that they can be removed from the fuel assembly, if necessary.

The cylindrical fuel pellets are sintered, high density ceramic with a dish at each end. The edges of the pellets have chamfers that ease the loading of the pellets into the rod, and the dish and chamfer help reduce the tendency for the pellets to assume an hourglass shape during operation. Pellet enrichments may be as high as 4.95 weight percent U-235 with ± 0.05% tolerance.

The fuel rod design can also utilize axial blanket and gadolinium fuel configurations. Axial blanket fuel rods can contain up to seven zones: a central zone of enriched UO_2 pellets or UO_2 plus Gd_2O_3 pellets, two outside enriched UO_2 zones above and below the central zone, two cutback zones of enriched UO_2 pellets above and below the outside zones, and two axial blanket zones at each end of the stack. The axial blanket region consists of sintered UO_2 pellets with a lower U-235 enrichment. The gadolinia serves as a burnable poison to control power peaking or core reactivity, and the fuel pellets containing gadolinia are typically located in the central zone.

Table 4.2-1 shows the major fuel rod design parameters. The fuel rod dimensions presented are subject to change, while meeting the design bases, as additional operating data are acquired. Additional fuel rod and component parameters are provided in the Fuel Assembly Mechanical Design Topical Report (Reference 1).

4.2.2.9 Rod Cluster Control Assemblies Description

Each AREVA NP HARMONI™ RCCA consists of a group of 24 individual control rods fastened to a spider assembly (see Figure 4.2-12—Rod Cluster Control Assembly). The individual rods (see Figure 4.2-13—RCCA Control Rod) consist of an absorber rod of 80 weight percent Ag, 15 weight percent In, and 5 weight percent Cd sealed within a 316L stainless steel cladding tube to protect the absorber from the coolant. The tube is plugged and welded at each end. The exterior of the rods (except the uppermost welded region) is ion-nitrided to produce a wear resistant surface to minimize mechanical damage from the fuel assembly and reactor internals. The top ends of the rods are securely fastened to a spider using a threaded and pinned joint. The upper end plug is designed with a flex joint which provides the ability to accommodate misalignment between the rods and the fuel assembly.

The RCCA spider (Figure 4.2-14—RCCA Spider) is in the form of a welded and brazed array of vanes and fingers on a hub; however this does not preclude other configurations, such as an integrally-cast spider and vanes. A spring is located in the lower part of the hub, and is designed to absorb the kinetic energy of the RCCA and driveline following reactor trip. The spring is preloaded and maintained within the hub by a retaining ring and tension bolt. The RCCA is coupled to the control rod driveline through the coupling section machined within the top part of the hub. During a refueling outage or after reactor trip, the retaining ring rests on the fuel assembly top nozzle.

Table 4.2-3—RCCA, Source Assembly, and TPA Component Materials provides a summary of the materials used for the RCCA and the other fuel system components (described below). These materials are identical to current 17x17 RCCA components supplied to U.S. PWRs. Based on past experience, these materials may be reliably used in PWR environments.

Table 4.2-4—RCCA Characteristics and Design Parameters provides the nominal dimensions, descriptions, and weights for the RCCA, spider, and control rods. Table 4.2-5—Control Component Mechanical Strength lists the material properties for the RCCA structural components. For ASME Code materials, other physical properties are taken from the Part D of the ASME Code, Section II (Reference 10).

4.2.2.10 Stationary Control Component Assemblies Description

Several types of stationary core components reside within the non-RCCA fuel assemblies. There are three basic types of SCCA component: thimble plug assemblies, primary source assemblies, and secondary source assemblies. Of the 241 fuel assembly locations within the U.S. EPR core, 89 interface with RCCAs and the remaining 152 interface with an SCCA of some type.

The purpose of TPAs, shown in Figure 4.2-15—Thimble Plug Assembly, is to restrict coolant bypass flow through the fuel assembly guide tubes and to guide the incore instrumentation probes into the fuel bundle. The U.S. EPR uses 152 TPAs of three different configurations:

- *Type 1:* These TPAs have 24 thimble plugs. Type 1 TPAs are used in non-instrumented fuel assemblies. The initial number of Type 1 TPAs depends on the number of source assemblies used, and is plant-specific.
- *Type 2:* These TPAs have 23 thimble plugs and one incore lance guide ring. There are 28 Type 2 TPAs and they are used in instrumented fuel assemblies.
- *Type 3:* These TPAs have 22 thimble plugs and two incore lance guide rings. There are 12 Type 3 TPAs and they are used in instrumented fuel assemblies.

The spider assemblies for the different TPA configurations are essentially identical, except for the number of incore guide rings (none, one, or two) and the guide ring positions (see Figure 4.2-16—TPA Spider Showing the Guide Ring Positions). There are six possible orientations for the guide rings (the four corner positions for the one-ring TPA, and the two orthogonal positions for the two-ring TPA). The TPA plugs that attach at the non-guide ring locations are solid 308L stainless steel rods machined with a bullet nose on the bottom end and with a threaded upper end for connecting to the spider fingers.

Primary source assemblies (see Figure 4.2-17—Primary Source Assembly) contain Cf-252, a controlled neutron source for reactor startup during the first, and possibly second, operating cycle. Primary source assemblies use an identical spider design as Type 1 TPAs. They support one primary neutron source rod, while the other 23 rod locations support thimble plugs for bypass flow restriction. As the startup sources are no longer required, the primary source assemblies are eventually replaced by Type 1 TPAs. The number of primary source assemblies is plant-specific.

Secondary source assemblies (see Figure 4.2-18—Secondary Source Assembly) are used as controlled neutron sources for reactor startup following the first cycle of operation, and are generally used for two to three operating cycles. The exact number of cycles and the number of source assemblies is plant-specific. Secondary source assemblies use an identical spider design as Type 1 TPAs, with 20 short and four long secondary source rods. Secondary source assemblies start with nonradioactive antimony-beryllium (Sb-Be) which becomes activated during the first operating cycle. The activated Sb-Be material provides a controlled neutron source for subsequent cycles. Similar to the primary source assemblies, the secondary source assemblies are ultimately replaced by Type 1 TPAs.

Primary and secondary source rods use 316L cladding tubes and 308L welded end plugs for encapsulation. The primary neutron source (Cf-252) is further encapsulated in a multiple-walled vessel placed within the cladding, and positioned vertically with solid alumina spacers. The secondary source rods utilize cold-pressed Sb-Be pellets without spacers. The primary and secondary source rods are illustrated in Figure 4.2-19—Primary Neutron Source Rod and Figure 4.2-20—Secondary Neutron Source Rod.

The spiders used for the TPAs, primary source assemblies, and secondary source assemblies are very similar. The spiders consist of a central hub and array of 16 vanes integrally machined from wrought 304L stainless steel. Each vane includes either one or two fingers to attach either thimble plugs or source rods, using stainless steel, threaded, bullet-head nuts. A separate hub is welded to the top of the machining, which serves as a positive stop for the spider assembly spring on one end, and internal (coupling) grooves that interface with handling equipment on the other end. Each spider assembly is stationary, situated between the upper core plate and the fuel assembly top nozzle. A hold-down spring precludes a solid load path between the upper core plate and the fuel assembly top nozzle, and holds down the SCCA while accommodating fuel assembly growth and thermal expansion.

Figure 4.2-21—Control Template, shows the control template that is used to verify the dimensional compatibility of the SCCAs with the fuel assembly guide thimble locations. Table 4.2-6—SCCA Characteristics and Design Parameters, provides a summary of selected SCCA components. Key features of the source rods are listed in Table 4.2-7—Rod Parameters for Primary and Secondary Source Assemblies.

4.2.3 Design Evaluation

The U.S. EPR fuel rods, fuel assemblies, and control components conform to the guidance of the Standard Review Plan, Section 4.2 (Reference 11).

The design evaluation begins by identifying the limiting fuel rods. The limiting fuel rods are those of which predicted performance provides the minimum margin to the

design criteria. The limiting rod may be the lead burnup rod within a fuel region, or it may be the maximum power rod. Typically, no single rod is limiting for all design criteria.

After identifying the limiting rods, analyses are performed to consider other factors, including rod operating history, model uncertainties, and dimensional variations. To verify adherence to the design criteria, the evaluation also considers the effects of power transients. The performance of the fuel during AOOs, PAs, and anticipated transients without scram (ATWS) is also presented in Chapter 15 (GDC 10).

4.2.3.1 Cladding

4.2.3.1.1 Vibration Analysis

A bending stress is induced in the cladding as a result of coolant flow causing the rod to vibrate against the spacer grids. This flow-induced vibration bending stress is taken into account in the cladding stress analysis of Section 4.2.3.1.2.

Extensive flow and wear tests were performed on the fuel assembly design. The first phase of the testing was performed in a full-scale test channel where both axial and cross flow velocities were imposed on a fuel assembly. The assembly (grid) and rod responses to the various flows were measured and reported. The next phase was an autoclave wear test of a short two-span rod segment, supported by three grids of varying design and conditions. The measured rod amplitudes from the full-scale flow test are imposed on the rod segment in the autoclave wear test with different durations up to 1000 hours with recordings made of possible wear.

Vibration and wear testing, as well as the operating experience with HTP grids with M5™ rods, show that the U.S. EPR design has significant margins against excessive fretting wear for the expected operating conditions. The testing concluded:

- The bottom span experiences the most turbulent excitation, which is mostly from cross-flow.
- The cross-flow imposed during these tests was nearly twice as large as the maximum values expected in the reactor.
- Very conservative (large) bounding rod motions due to these very large cross-flows were imposed during the wear tests and no excessive wear was produced.
- The extensive operating experience supports applying these test results and conclusions to the U.S. EPR.

See Section 4.2.3.5.7 for additional details of fuel rod fretting evaluations.

4.2.3.1.2 Fuel Rod Internal and External Pressure and Cladding Stresses

The following types of stresses were analyzed in the cladding stress analysis:

- Pressure Stresses: These are membrane stresses from external and internal pressure on the fuel rod cladding.
- FIV: These are longitudinal bending stresses from vibration of the fuel rod caused by coolant flow around the rod.
- Ovality: These are bending stresses from external and internal pressure on the fuel rod cladding that is oval. This does not include the stresses resulting from creep ovalization into an axial gap.
- Thermal Stresses: These are secondary stresses that arise from the temperature gradient across the fuel rod during reactor operation.
- Fuel Rod Growth Stresses: These secondary stresses are from the fuel rod slipping through the spacer grids. These may be caused by the fuel assembly expanding more than the fuel rod due to heat-up, or from fuel rod growth from irradiation.
- Fuel Rod Spacer Grid Interaction: These are secondary stresses from contact between the fuel rod cladding and the spacer grid.
- Spring Force Stress: This is a primary membrane stress; the axial stress is load dependent.

Classifications of stresses are as follows (loading condition: stress category):

- Pressure Stresses: $P_{m,}$ Primary membrane.
- Ovality Stresses: $P_{b,}$ Primary membrane bending.
- Spacer Grid Interaction: Q, Secondary.
- FIV: $P_{b,}$ Primary membrane bending.
- Thermal: Q, Secondary.
- Differential Rod Growth: Q, Secondary.
- Plenum Spring Force: $P_{m,}$ Primary membrane.

The fuel rod cladding was analyzed for the stresses induced during operation using the approved methodology of Reference 2. Conservative values are used for cladding thickness, oxide layer buildup, external pressure, internal fuel rod pressure, differential temperature, and unirradiated cladding yield strength. The fuel rod stress analysis calculates the worst-case cladding stress state based on the thinnest cladding wall and largest cladding ovality. The likelihood of these two conditions occurring at

the same location on the cladding is remote; therefore, the consideration of these two conditions together to calculate the cladding stress state is conservative. The analyses of the fuel rod cladding stresses demonstrated positive margins for all operating conditions. The cladding stress safety margins are presented in the Fuel Assembly Mechanical Design Topical Report (Reference 1).

Analysis shows that fuel rod cladding buckling will not occur. Two critical buckling pressures, P_{cr} and P_{yp}, are calculated. P_{cr} is the bifurcation buckling pressure of a perfectly circular shell and is calculated to check the elastic stability of the cladding. P_{yp} is the pressure at which the cladding extreme fiber is loaded beyond the yield point and it accounts for cladding initial ovality. The maximum differential pressure is less than the buckling pressure and the critical pressure, thereby proving that the cladding will not buckle.

The fuel rod internal pressure is determined using the COPERNIC computer code (Reference 6) and the methodology defined in Reference 7. The results indicate the fuel rod can attain the design maximum burnup of 62 GWD/MTU approved in Reference 5. Inputs to the analysis included a power history that bounded the operation of any individual rod, and also worst-case manufacturing variations as allowed by the fuel rod specifications. On a cycle-specific basis, should peak rod powers violate the envelope, resulting in predicted pressure greater than the license limit, acceptable fuel rod pressure results can be demonstrated by utilizing fuel rod specific power histories and fuel assembly as-built manufacturing data.

4.2.3.1.3 Potential for Chemical Reaction

Reference 2 confirms that M5™ fuel rod cladding resists corrosion. From previous irradiation experience with this cladding type, the corrosion has been found to be significantly less than the corrosion of low-tin zirconium alloy cladding. Using the COPERNIC computer code (Reference 6), the maximum predicted oxide thickness is predicted to be much less than the limit established in the Extended Burnup Topical Report (Reference 5). Bounding power histories were used in predicting the oxide thickness. The maximum predicted oxide thickness is provided in Reference 1.

The absorption of hydrogen by the cladding is minimized in AREVA NP fuel rods by tight controls on the moisture and hydrogen impurities in the rod during fabrication. Cleaning and drying of the cladding and careful moisture control of the fuel pellets are used to minimize the total hydrogen within the fuel rod assemblies. These methods for preventing hydriding have been approved in Reference 2 and the specific hydrogen content limit of the M5™ cladding is provided in Reference 1.

4.2.3.1.4 Fretting and Crevice Corrosion

The evaluation method for fretting wear for the M5™ cladding is described in Reference 2 and the fretting evaluation is addressed in Section 4.2.3.1.1.

PWR operating experience has shown that crevice corrosion is not a likely corrosion mechanism for zirconium alloy cladding material. In general, zirconium alloys are very resistant to crevice corrosion. In addition, typical PWR coolant chemistry specifications impose tight controls for dissolved oxygen and chlorine, the contaminants that are often associated with crevice attack. For the U.S. EPR reactor coolant system (refer to Section 5.2, Table 5.2-3), the control limits for oxygen and chlorine are five and 10 ppb, respectively.

4.2.3.1.5 Stress-Accelerated Corrosion

Stress corrosion cracking is addressed in the M5™ Topical Report (Reference 2).

4.2.3.1.6 Cycling and Fatigue

The fuel rod cladding was analyzed for the total fatigue usage factor using the methodology approved in Reference 2 and the procedure outlined in the ASME Code (Reference 4). AREVA NP tests have determined the fatigue performance of M5™ cladding. These tests have shown similar fatigue endurance performance for recrystallized (RXA) cladding (including M5™) as compared to Zircaloy-4, with the lower yield strength of the RXA claddings limiting the applied stresses. The values for alternating stress (S_{alt}) versus number of cycles (N) are well enveloped by the standard O'Donnell and Langer design fatigue curve (Reference 12). A fuel rod life of eight years and a vessel life of 60 years are assumed. The fuel rod cladding will, therefore, experience 13 percent of the number of transient cycles the reactor pressure vessel will experience.

All expected normal operating, upset, and test transients were evaluated to determine the total fatigue usage factor experienced by the fuel rod cladding. These transients are summarized in the Fuel Assembly Mechanical Design Topical Report (Reference 1). In accordance with the ASME Code (Reference 4), faulted conditions are not included in the fatigue evaluation. Conservative inputs in terms of cladding thickness, oxide layer buildup, external pressure, fuel rod internal pressure, and differential temperature across the cladding were assumed. The results of the fatigue analysis for the U.S. EPR fuel rod show that the cumulative fatigue usage factor is well below the allowable limit of 1.0.

4.2.3.1.7 Material Wastage Attributable to Mass Transfer

Cladding oxidation usually results in crud buildup. An oxide thickness limit has been established in the Extended Burnup Topical Report (Reference 5), and the predicted

corrosion is significantly lower than the established limit. Because crude formation occurs in part from cladding oxidation, the M5™ cladding will have less crud buildup, even with other crud buildup factors remaining the same. Therefore, material wastage from mass transfer is greatly reduced.

4.2.3.1.8 Rod Bowing Attributable to Thermal, Irradiation, and Creep Dimensional Changes

Rod bowing is addressed in Section 4.2.3.5.6.

4.2.3.1.9 Consequences of Power-Coolant Mismatch

The consequences of power-coolant mismatch are addressed in Section 4.4.

4.2.3.1.10 Irradiation Stability of the Cladding

Considerable operating experience using M5™ cladding has proven its irradiation stability. The effects of irradiation on the mechanical integrity of the cladding has been accounted for using the approved COPERNIC model (Reference 6) for performing the mechanical and thermal analyses, and the effects are shown to be acceptable for the currently approved burnup limit of 62 GWD/MTU established in the Extended Burnup Topical Report Reference 5.

4.2.3.1.11 Creep Collapse and Creepdown

The computer code CROV, a creep ovalization analysis program developed and certified for AREVA NP fuel rods, is used to evaluate the resistance of the U.S. EPR fuel rod cladding to creep collapse. Use of the CROV code in performing the creep collapse analysis for M5™ cladding has previously been approved in the M5™ Topical Report Reference 2. Inputs to the analysis include differential pressure, temperature gradients, and fast flux. The enveloping power histories from the COPERNIC thermal-hydraulic analysis (Reference 6) are used to initialize the creep collapse code. As discussed in Reference 2, the creep rate of M5™ is approximately 50 percent slower than Zircaloy-4; therefore, a multiplier of 0.5 or higher (for conservatism) is applied to the CROV input for the M5™ analysis.

The following conservatisms were used in determining creep collapse over the life of the fuel rod:

- Minimum fuel rod pre-pressure.
- No fission gas release.
- A worst-case or enveloping power history.
- Worst-case cladding dimensions.

- Bounding value for cladding thickness.
- Bounding value for cladding ovality.

Fuel rod creep collapse is determined when either of the following happens:

- The rate of creep ovalization exceeds 0.1 mil/hr.
- The maximum fiber stress exceeds the unirradiated yield strength of the cladding.

Using the methodology described above, the fuel rod creep collapse lifetime was shown to be greater than the maximum design burnup of 62 GWD/MTU defined in Reference 5.

4.2.3.1.12 Cladding Strain

The cladding strain evaluation is discussed in the Fuel Assembly Mechanical Design Topical Report (Reference 1). The calculated linear heat rate for transients that induce one percent cladding strain do not limit the plant operation and are much greater than the maximum transient the fuel rod is expected to experience.

4.2.3.1.13 Pellet-Cladding Interaction

The criteria for transient-induced cladding strain and no centerline fuel melting are used to show an acceptable fuel rod design and are much greater than the maximum transient the fuel rod is expected to experience. This method has been previously approved in the Extended Burnup Topical Report (Reference 5).

4.2.3.2 Fuel

4.2.3.2.1 Dimensional Stability

Fuel pellet dimensional stability is provided by a rigorous quality inspection program that is used for AREVA NP PWR fuel pellets. Pellets are tested for resinter behavior according to criteria stipulated in the pellet specifications. Pellets are also inspected for such abnormalities as discoloration, inclusions, pits, unground areas, cracks, and chips. One hundred percent of the pellets are measured for diameter. To maintain the integrity of the fuel, the other dimensional attributes are measured based on a statistical sampling over the course of pellet grinding and inspection.

4.2.3.2.2 Potential for Chemical Interaction

Standard testing is performed to verify pellet stoichiometry (oxygen-to-uranium ratio), uranium content, and isotopic content (U-234, U-235, U-236, and U-238). For burnable absorber rods, gadolinia content is also measured. Microstructural examinations for grain size and internal porosity provide controls for limiting fission gas release.

Pellet hydrogen and fluorine content are tightly controlled to minimize the potential for hydride blister formation on the cladding inner surfaces. Introduction of unacceptable levels of hydrogen from contamination sources is further prevented by implementation of visual inspections of pellets immediately following grinding and immediately prior to loading into fuel rods. Testing for nitrogen, carbon and oxygen verify sorbed gas limits within the pellets. Testing for elemental impurities and calculation of the equivalent boron content is also performed to prevent unwanted neutron capture by tramp elements.

4.2.3.2.3 Thermal Stability

Fuel melting does not occur during normal operation or AOOs (Reference 2). The COPERNIC fuel performance computer code (Reference 6) is used for the centerline fuel melt analysis. COPERNIC determines the local linear heat rate throughout the fuel rod lifetime that results in centerline temperatures exceeding a T_L, which is a limit value chosen such that a 95 percent probability exists at the 95 percent confidence level that centerline melting will not occur.

The local linear heat rate throughout the rod lifetime determined in the centerline fuel melt analysis is used as input to determine the limiting conditions for operation and reactor set points. During normal operation and AOO, the fuel will not melt because the linear heat rate does not exceed the limit established in the centerline melt analysis.

4.2.3.2.4 Irradiation Stability

The irradiation stability of the fuel is confirmed by performing analyses using the COPERNIC code (Reference 6) that analyzes the fuel throughout the life of the fuel rod.

4.2.3.3 Fuel Rod Performance

4.2.3.3.1 Fuel Rod Performance Predictions

COPERNIC is the fuel rod design computer code used to perform thermal and mechanical analyses to accurately simulate the behavior of a fuel rod during irradiation, and to verify the fuel rod design meets design and safety criteria. COPERNIC calculates fuel melting, fuel rod internal gas pressure, cladding strain, cladding peak oxide thickness, and initialization parameters for the cladding creep collapse. The following phenomenological models are utilized in the COPERNIC code, as described in Reference 6:

- Radial power distribution.
- Fuel and cladding temperature distribution.

- Burnup distribution in the fuel.
- Thermal conductivity of the fuel, cladding, cladding crud, and oxidation layers.
- Densification of the fuel.
- Thermal expansion of the fuel and cladding.
- Fission gas production and release.
- Solid and gaseous fission product swelling.
- Fuel restructuring and relocation.
- Fuel and cladding dimensional changes.
- Fuel-to-cladding heat transfer coefficient.
- Thermal conductivity of the fuel rod internal gas mixture.
- Thermal conductivity in the Knudsen domain.
- Fuel-to-cladding contact pressure.
- Heat capacity of the fuel and cladding.
- Growth and creep of the cladding.
- Rod internal gas pressure and composition.
- Sorption of helium and other fill gases.
- Cladding oxide and crud layer thickness.
- Cladding-to-coolant heat transfer coefficient.

4.2.3.3.2 Fuel-Cladding Mechanical Interaction

Fuel-cladding mechanical interaction is addressed in Section 4.2.3.1.13.

4.2.3.3.3 Failure and Burnup Experience

Failure and burnup history for fuel rods and fuel assemblies are presented in the Fuel Assembly Mechanical Design Topical Report (Reference 1).

4.2.3.3.4 Fuel and Cladding Temperatures

Fuel and cladding temperature analyses are described in Section 4.4.

4.2.3.3.5 Potential Effect of Temperature Transients

The potential effect of temperature transients on waterlogged fuel rods has been evaluated for the U.S. EPR fuel rods. The evaluation concluded that cladding rupture due to a waterlogged condition is a very low probability, based primarily on the nominal 96 percent theoretical density (TD) fuel pellets. Test results showed that fuel rods with pellets of 90 percent TD were unlikely to swell and rupture. Normal operating parameters for the U.S. EPR are expected to be similar to the current generation of plants. Differences in power ramp rates would not be of a magnitude to exceed the threshold values determined to be necessary to result in cladding swelling and rupture from a waterlogged condition. Thus, the impact of waterlogged fuel rods will be no more adverse for the U.S. EPR than it is for the current generation of plants.

4.2.3.3.6 Analysis of Temperature Effects

Section 4.4 discusses the impact of temperature effects during anticipated operational transients and the effect from fuel rod bow, as well as other fuel rod thermal design bases.

4.2.3.4 Spacer Grids Evaluation

The maximum impact load on the spacer grids due to combined SSE and LOCA at BOL conditions is provided in the Fuel Assembly Mechanical Design Topical Report (Reference 1). An intermediate grid location on a peripheral fuel assembly within an intermediate length row configuration produced the maximum impact force. The combined loads for seismic and LOCA resulted in no grid deformation, based on the BOL hot allowable grid load established by hot testing in Reference 1.

The predicted spacer grid impact loads for SSE conditions were within the allowable elastic load limits, resulting in no plastic deformation of the spacer grid geometry. Since the grids remain elastic, core coolable geometry is maintained for faulted loads (GDC 35 and 10 CFR 50.34) and deformed fuel assembly conditions did not need to be evaluated.

Since the spacer grid loads are within the elastic limit for the SSE, these results also satisfy the OBE requirements that the assembly or components not exceed the applicable yield limit (the magnitude of the OBE is one-half the magnitude of the SSE). Hence a separate OBE analysis is not required.

4.2.3.4.1 Spacer Grid Dimensional Stability

The spacer grids are suitable for use in the U.S. EPR both chemically and thermally, and they comply with applicable design criteria for environmental effects, including irradiation and corrosion. This conclusion is based on PWR operating experience with M5™ HTP and Alloy 718 HMP grids in combination with M5™ fuel rods and M5™

guide tubes, and with the M5™ material and generic HTP grid evaluations that have been approved by the NRC as provided in the References 2, 3, and 9, and Generic Mechanical Design Report High Thermal Performance Spacer and Intermediate Flow Mixer (Reference 13).

4.2.3.4.2 Spring Loads for Grids

The forces required to slip the grid relative to the fuel rods were measured at BOL conditions. These data, which represent the friction force between the grids and fuel rods, were used as input in analytical models of the fuel assembly. Typical BOL slip loads at room temperature for HTP grids and unrelaxed HMP grids are presented in Reference 1.

4.2.3.5 Fuel Assembly Design Evaluation

The U.S. EPR fuel assembly design has been evaluated to demonstrate that the fuel assembly satisfies the requirements outlined in the Standard Review Plan (Reference 11). The fuel assembly design evaluation, including the fuel rods, is detailed in Reference 1 in relation to the Standard Review Plan criteria for fuel system damage mechanisms, fuel rod failure mechanisms, and fuel coolability. A summary level description of the evaluation is provided in this FSAR section. A similar summary of the evaluations for the fuel rod design is also presented above in Section 4.2.3.1, Section 4.2.3.2, and Section 4.2.3.3.

Methodologies and models specific to the M5™ application are provided in References 2, 3, and 9. Methodologies for the fuel assembly faulted structural evaluations are described in References 8 and 9. The design bases follow those established for the Mark-BW fuel assembly in the Mark-BW Mechanical Design report (Reference 14), the Advanced Mark-BW Fuel Assembly Mechanical Design report (Reference 15) and for the generic HTP grids (Reference 13).

The results of the analyses are applicable to fuel assembly operation in 17x17 U.S. EPR fuel plants. The analyses were performed for a peak fuel rod burnup of 62 GWD/MTU.

4.2.3.5.1 Fuel Assembly Structural Design Evaluation

The design criterion for structurally evaluating the U.S. EPR fuel assembly is that stress intensities shall be less than the stress limits based on ASME Code, Section III criteria (Reference 4).

The structural design requirements for the U.S. EPR fuel assembly are mostly derived from AREVA NP design and incore operating experience with similar designs. The design bases and design limits for the U.S. EPR fuel assembly are essentially the same as those for previously licensed and approved fuel assembly designs such as those approved in References 14 and 15. The requirements are consistent with the

acceptance criteria in the Standard Review Plan (Reference 11). Stress intensities, and in some cases Von-Mises stresses, were shown to be less than the applicable stress limits. Code Level A criteria are used for normal operating conditions and code Level D criteria are used for the LOCA and seismic (i.e., faulted) analyses.

The fuel assembly component evaluations showed that primary stresses and primary plus secondary stresses are lower than the material allowable stresses for both normal operation and faulted conditions for all evaluated components. The evaluation of components for faulted conditions considered the square root of the squares summed combination of the LOCA and SSE loads.

The fuel assembly components that were evaluated include:

- Guide tubes: The guide tubes were shown not to buckle but remain elastic, thereby ensuring control rods can be inserted during normal operation. A positive guide tube buckling safety margin was determined for axial loading for the hot zero power (HZP) condition. The HZP condition was determined as the limiting normal operating case for compressive loading compared with hot full power (HFP) operation. RCCA impact loads due to SCRAM operations were considered. The critical buckling load was determined by a finite element model using large deflection criteria to identify the onset of buckling. A small initial lateral deflection was imposed on the fuel assembly model at mid-height to account for potential reduction in the critical load due to fuel assembly bow. The HZP power load distribution was incrementally scaled to the point where large deflections indicative of the onset of buckling were calculated to occur. A large margin against buckling was demonstrated. Guide tube corrosion tolerances, and temperature effects were considered. Additionally, midspan nodal deflections between grids for HZP were shown to be very small, such that the calculated margin against inelastic behavior is accompanied by limited small displacements, thereby providing a supplemental demonstration of control rod insertion under HZP conditions.

- Spacer grids: The spacer grids were shown to remain elastic during normal operation and faulted conditions. The mechanical design bases of the U.S. EPR spacer grids were confirmed through a series of tests on prototype 17x17 M5™ HTP grids as discussed in Section 4.2.4.3.2.

- Bottom nozzle: The evaluation for normal operating conditions was performed in accordance with Subsection NG-3228.4 of the ASME Code (Reference 4) using a design limit of 44 percent of the maximum cold test load obtained by testing. Bottom nozzle testing is described in Section 4.2.4.3.3. The limit based on the maximum test load is further discounted for operating temperature conditions. Axial loading only is considered because the normal operating loads on the bottom nozzle are applied axially by the guide tubes. The maximum normal operating load used in the evaluation was conservatively taken as the limiting hold-down spring load from the fourth pump startup case plus the dry weight of the fuel assembly with no flow lift considered. The limiting hold-down spring load is taken for the upper tolerance limit (UTL) guide tube growth derived in the

evaluation of the margin against flow liftoff.

The evaluation of the bottom nozzle for faulted operating conditions was performed in accordance with Appendix F, Paragraph F-1440(a) of the ASME Code (Reference 4) using a design limit of 80 percent of the maximum cold test load. The limit based on the maximum cold test load is further discounted for normal operating temperature evaluations. The maximum normal operating load used in the evaluation included moment loads plus the assembly weight plus LOCA plus SSE axial loads. Moment loads were considered by calculating the axial load equivalent of the moment couples created by the position of the guide tubes in relation to the center of the bottom nozzle. Margin to the design limit was demonstrated.

- Top nozzle: The top nozzle structure was evaluated for normal operating and shipping and handling loads using an ANSYS finite element analysis model. A limiting case was evaluated for normal operating loads that included maximum hold-down spring load established by the assembly liftoff evaluation (Section 4.2.3.5.5) and the weight of the fuel assembly.

- Hold-down spring: Stress analysis of the U.S. EPR fuel assembly hold-down spring examined stresses, strains, and fatigue usage to confirm that it does not break. The evaluation confirmed that all of the ASME Code criteria are satisfied.

  The spring stresses were treated as secondary stresses since the hold-down spring stresses are controlled by the total separation between the lower and upper core plates. However, some fraction of the spring force is necessary to hold the fuel assembly down (i.e., to satisfy internal equilibrium) and therefore a portion of' the total stress was treated as primary. The primary stress criterion is met because failure of the structure due to primary stresses cannot occur due to the geometry of the spring leaves and top nozzle. The secondary stress limits were satisfied by performing a plastic analysis to Subsection NG-3228.1 of the ASME Code (Reference 4). The hold-down springs are shown to shake down to elastic action as required. The maximum normal operating loading bounds the faulted condition when the head is bolted on and the fourth pump is started (i.e., at cold conditions), thus satisfying the normal operating conditions also satisfies the faulted condition criterion. The known spring displacements were converted to stresses to demonstrate the criterion was met.

- QD Connection at top nozzle: Hot compression tests of the upper QD connection (see Section 4.2.4.3.1) showed that the mechanical strength of the QD connector is limited by the performance of the guide tube and not by the welded connection between the sleeve and guide tube. Using Article NG-3228.4 of the ASME Code (Reference 4), it was shown that the evaluated maximum load on the connector is less than the load design limit of 44 percent of the maximum cold test load.

- Guide Tube Assembly End Plug Connection to Bottom Nozzle: The Von Mises stress based on the initial preloaded condition of both the fastener and the end plug were evaluated to be within design limits. These stresses are then adjusted to reflect the addition of handling loads and these were also found to be within the design limits. And finally, the fourth pump startup and HFP conditions of the end

plug are determined from the initial preloaded condition and determined to be within design limits. The coefficient of thermal expansion of the fastener and the bottom nozzle are greater than for the threaded plug. Therefore, preload is lost during system warm-up because the axial growth of the fastener moves the plug further than the plug expands. In addition, the differences in thermal expansion coefficients introduce large hoop stresses, exceeding the yield point of the material within the end plug. Since these thermal stresses are strain limited, they shake down to elastic action without strain rupture of the end plug or loss of function after the initial heating cycle. The end plug was evaluated on a plastic basis in which a design margin was calculated based on the strain rupture limit of the end plug.

- Fuel Rod Cladding: The structural evaluation of the fuel rod cladding for normal operation is discussed in Section 4.2.3.1.2 and Section 4.2.3.1.6. The evaluation confirmed that all of the ASME Code criteria are satisfied and that a fatigue usage factor of less than 1.0 can be demonstrated.

  The evaluation of the fuel rod cladding for faulted conditions considers the LOCA and SSE loads superimposed on the normal operating loads. The evaluation confirmed that all of the ASME Code criteria are satisfied.

In accordance with the Standard Review Plan criteria in Section 3.7.3 of Reference 11, structurally significant fuel assembly components were also evaluated for normal operating plus fatigue stress cycling of five OBE events followed by one SSE event of 10 maximum stress cycles per event. The normal operating fatigue cycle counts from the plant RCS design specification were used to establish a count of the RCS design transients to be evaluated. The RCS life events were adjusted to eight effective full power years per fuel assembly for determining fuel component cycle counts. In the fatigue evaluations for earthquakes, an SSE stress cycle is used as an enveloping stress cycle for all earthquake events. A total of 60 SSE stress cycles were considered. In all cases a total fatigue usage factor of less than 1.0 was demonstrated, considering the full life stress cycles for normal operation and up to 60 SSE stress cycles.

4.2.3.5.2 Analysis of Combined Shock and Seismic Loading

The structural integrity of the fuel assembly has been verified to withstand seismic and LOCA events under BOL hot conditions using the methodology in the Mark-C LOCA-Seismic Topical Report (Reference 8). The fuel assembly will maintain safe operation following an OBE, an SSE, and a LOCA by maintaining the dimensions needed for control rod insertion and a coolable geometry consistent with emergency cooling systems and with safety analyses. The horizontal and vertical loads on the components were first determined with analytical models, and these loads were then combined in an evaluation of each component.

The horizontal component of the faulted analysis determines the structural integrity of the U.S. EPR fuel assembly in the horizontal direction. Loading conditions were

evaluated at BOL and EOL for an SSE, LOCA, and a combined seismic and LOCA event.

U.S. EPR fuel assembly models were benchmarked using properties established through testing. Fuel assembly models were combined to represent row configurations of fuel assemblies in the core. Row models with seven to 17 assemblies were created. Typical seismic SSE displacement time histories at the lower core plate, upper core plate, and upper end of the heavy reflector were evaluated. The LOCA lateral displacements evaluated corresponded to a worst-case attached pipe break based on leak-before-break. The SSE and LOCA time histories were applied to the reactor core model. The fuel assembly response was determined per the methodology described in Reference 8.

The maximum grid impact forces that were obtained for SSE and SSE plus LOCA conditions for a full-core configuration of U.S. EPR fuel assemblies were less than the allowable limits established by testing, as discussed in Section 4.2.3.4.

Other fuel assembly components were evaluated for combined assembly vertical and horizontal loads under SSE plus LOCA conditions and found to be acceptable against the criteria for core coolable geometry, and the component stresses were shown to be less than the allowable limits based on ASME Code, Section III criteria. The core coolable geometry will be maintained for all the faulted loads and the component stress intensities were less than the allowable limits.

Since the spacer grid loads are within the elastic limit for the SSE, these results also satisfy the OBE requirement that the assembly or components not exceed their applicable yield limit (usually the magnitude of the OBE is half the magnitude of the SSE). Hence a separate OBE analysis is not required.

The fuel assembly was evaluated for the vertical LOCA condition with a finite element lumped mass model similar in approach to the model provided in the Mark-C LOCA-Seismic Topical Report (Reference 8) but with applicable modifications to the elements to represent the U.S. EPR design parameters. Axial loads on the fuel assembly components from the LOCA were analyzed using the ANSYS general finite element code. Fuel assembly axial stiffness properties and drop impact loads were obtained from testing and were used to benchmark the fuel assembly axial model. The example evaluation used vertical core force time histories that correspond to bounding attached pipe breaks based on leak-before-break methodology.

The fuel assembly component stress analyses for faulted conditions were performed using combined axial and lateral loads generated by seismic and LOCA loading analyses. SSE and SSE plus LOCA loading were used for the component analyses. The loads for the worst-case LOCA break were conservatively combined with those of the SSE to determine maximum fuel assembly loads. The component stress intensity limits

for the components were based on the Level D service limit of the Section III of the ASME Code.

The design margins indicate that the major components of the U.S. EPR fuel assembly meet the design criteria for the SSE and SSE plus LOCA loading events.

4.2.3.5.3 Load Applied in Fuel Handling

Both the fuel assembly and individual components were evaluated for structural adequacy for shipping and handling loads in the amount of 6g lateral and 4g in the axial direction. The evaluations resulted in positive design margins against the stress limits.

4.2.3.5.4 Axial Growth

4.2.3.5.4.1 Fuel Assembly Top Nozzle to Fuel Rod Shoulder Gap

A fuel assembly top nozzle-to-fuel rod shoulder gap allowance is provided that will maintain positive clearance during the entire assembly lifetime. The evaluation determined that a minimum fuel rod shoulder gap occurs at EOL hot conditions and considers the upper tolerance limit for fuel rod growth, minimum guide tube growth, and worst case tolerances on the length of the fuel rods and guide tubes. The evaluated minimum fuel rod shoulder gap is presented in the Fuel Assembly Mechanical Topical Report (Reference 1).

4.2.3.5.4.2 Fuel Assembly Top Nozzle to Reactor Internals Gap

A fuel assembly-to-reactor internals gap allowance is provided that maintains a positive core plate gap clearance throughout the entire life of the fuel assembly. The core plate gap allowance considers combined worst-case internals-fuel assembly differential thermal expansion and irradiation induced axial length changes to the guide tubes. The evaluation determined that a minimum fuel core plate gap occurs at EOL cold conditions and considered the upper tolerance limit guide tube growth and worst case tolerances on the length of the fuel rod and core plate separation. The evaluated minimum core plate gap is presented in Reference 1.

4.2.3.5.4.3 Fuel Assembly and Fuel Rod Growth Limits

U.S. EPR specific axial fuel assembly and fuel rod growth limits were developed for the following evaluations, which consider fuel assembly axial growth due to irradiation:

- Fuel assembly-to-reactor internals gap allowance.
- Fuel rod shoulder gap allowance.
- Verification of margin against flow liftoff (hold-down).

Operating experience regarding fuel assembly growth has been applied to the U.S. EPR fuel design. The U.S. EPR fuel assembly growth model was derived by the application of the empirical M5™ guide tube irradiation growth data. The data obtained to date, in conjunction with calculations, consider the specific EPR design attributes and M5™ free irradiation growth and creep as a function of temperature and stress. The calculation method was validated by benchmarking against existing M5™ growth data for the AREVA NP 12 ft Mark-BW fuel assembly.

The consideration of guide tube stress as defined by the governing design variables and loadings, in combination with correlations with the post-irradiation examination (PIE) growth, is appropriate in establishing the design criteria. The fuel assembly growth limits thereby established for the U.S. EPR design are provided in Reference 1.

The U.S. EPR fuel rod growth model was derived by the application of the empirical M5™ fuel rod irradiation growth data obtained to date by PIEs. The growth limits consider the statistical upper and lower limits of all the M5™ data collected for all fuel designs and operating conditions represented in the data. The fuel rod growth limits established for the U.S. EPR design are also provided in Reference 1.

4.2.3.5.5 Assembly Liftoff

The U.S. EPR fuel hold-down was evaluated to be capable of maintaining fuel assembly contact with the lower support plate during normal operating AOOs, except for the pump overspeed transient. The fuel assembly does not compress the hold-down spring to solid height for any AOOs and the fuel assembly top and bottom nozzles maintain engagement with reactor internals for all AOOs and PAs.

The fuel assembly lift evaluation was performed by comparing the hold-down force from the leaf springs and fuel assembly weight with that of the hydraulic forces at both normal operating conditions and pump overspeed conditions. The spring characteristics were determined by load deflection testing described in Section 4.2.4.3.4. Hydraulic forces were determined using the NRC-approved LYNXT code, as described in LYNXT: Core Transient Thermal-Hydraulic Program (Reference 16), which was used to determine the worst case flow lift forces. Spring plasticity and spring relaxation from irradiation were considered.

Flow conditions ranging from the fourth pump startup at 140°F to pump overspeed at 120 percent flow at full power conditions were considered. Although a pump overspeed event is not considered credible for the U.S. EPR design, the evaluation considers this case as enveloping with respect to the magnitude of the flow lift forces that are possible for any other AOO; therefore no other AOOs need to be evaluated. BOL and EOL conditions were also evaluated to consider the change in load paths and loads due to material relaxation.

A very conservative deterministic methodology was used to determine spring deflections and loads. This methodology uses the algebraic sum of extreme variations in core plate separation and fuel assembly growth and length when determining spring deflections and loads. This conservative method results in smaller margins than those that may be calculated using a statistical methodology. In the future, additional U.S. EPR hold-down evaluations may use the statistical hold-down methodology approved in the Codes and Methods Topical Report (Reference 3).

Using the deterministic evaluation approach, assembly liftoff during normal operating conditions will not occur, except for 120 percent pump overspeed conditions. The minimum margin to fuel assembly liftoff occurs at EOL, under HFP conditions assuming lower tolerance limit (LTL) fuel assembly growth, UTL core plate separations, and LTL fuel assembly length. For the 120 percent pump overspeed condition (not applicable but bounding) the fuel assembly will experience some liftoff. The liftoff will be minimal, and the hold-down spring deflection will be less than the worst-case normal operating cold-shutdown condition.

4.2.3.5.6 Fuel Rod Bow

Fuel rod bowing is evaluated with respect to the mechanical and thermal-hydraulic performance of the fuel assembly (Section 4.4). Although there is no specific mechanical design criterion for fuel rod bow, the design will follow the rod bow limits as established in Reference 5 and in Fuel Rod Bowing in Babcock and Wilcox Fuel Designs (Reference 17).

Because there are no domestic fuel rod bow data specific for fuel assemblies with HTP grids, AREVA NP has performed a comparative evaluation of the U.S. EPR fuel assembly with respect to existing fuel designs in order to trend future performance with respect to current bowing data. Key factors such as slip load, rod dimensions, span lengths, rod growth, and physics were evaluated.

The design slip load of the U.S. EPR HMP upper end grid is less than any other approved 17x17 designs. Because the upper end grid slip is 44 percent less than that of the lower end grid, the slip of the upper end grid will govern the performance of the assembly with regard to rod bow. Intermediate M5™ grid slip loads were not considered to be a factor because they will relax early in the first cycle of operation. The high degree of fuel rod rotational fixity afforded by HTP and HMP grid line contacts will significantly improve any adverse tendency for rod bow.

The influence of span length between spacer grids on rod performance will not be a factor because the average span lengths for the U.S. EPR design are shorter than that for 12 ft MK-BW designs for which PIE data are available. Likewise, the magnitude of flux applied to the U.S. EPR fuel rods is consistent with other core designs for which PIE data are available.

The lower growth characteristics of the M5™ advanced material that is used on the U.S. EPR can be expected to result in fuel rod bow behavior that is no more severe than the Zircaloy-4 clad fuel. The growth of M5™ for equivalent burnups across the entire range of the database has been demonstrated by irradiation experience to be consistently lower than Zircaloy-4 for each fuel design type, both domestically and in Europe.

In consideration of the PIE data and the comparative design feature evaluations (see Reference 1), AREVA NP has concluded that rod bow performance will be similar to that of other AREVA NP designs and that the rod bow correlations from References 5 and 17 are applicable to the U.S. EPR fuel assembly design, including consideration of extended burnup conditions.

4.2.3.5.7 Fuel Rod Fretting

The primary design criterion with regard to fuel rod fretting is that the design must limit fretting to preclude fuel rod failure. A supplemental criterion is that span average cross-flow velocities shall be less than 2 ft/s, as previously established in References 13, 14, and 15.

A full core analysis of the U.S. EPR fuel demonstrated span-average cross-flows less than 2 ft/s. The cross-flow velocities were determined using the NRC-approved LYNXT code per References 3 and 16, which established the flow and pressure drop characteristics of the U.S. EPR fuel assembly for full core implementation.

The U.S. EPR fuel rod fretting and wear performance is favorably based on the following tests and evaluations:

- Full scale 1000 hour endurance flow testing performed on a 12 ft fuel assembly design using Zircaloy-4 fuel rods and Zircaloy-4 HTP grids, which was the basis for evaluation and approval by the NRC for HTP grids in Reference 13.
- Favorable U.S. operating experience with 12 ft fuel assemblies incorporating both Zircaloy-4 and M5™ fuel rods and HTP grids.
- Full scale 1000 hour endurance flow testing on a 14 ft U.S. EPR prototype in the HERMES-P flow test facility (Reference 1). Extremely unfavorable rod support conditions and extremely large cross-flows were tested.
- Supplemental out-of-core life and wear and FIV testing using the PETER Loop Autoclave test methodology (Reference 1) accompanied by performance benchmarks against fretting performance of other designs.
- Negative results for specifically targeted tests for self-induced vibration modes performed with full-scale fuel assembly prototypes in two independent test facilities, namely the PETER Loop and HERMES facilities.

The basis for extending the fretting resistance of Zircaloy-4 HTP grids on Zircaloy-4 fuel rods demonstrated in Reference 13 to M5™ HTP grids and fuel rods is provided in Reference 2. The fretting resistance operating experience for 12 ft HTP fuel assemblies can also be extended to the U.S. EPR 14 ft assembly that is in other ways similar to existing 12 ft designs. Operating experience demonstrates that the fretting of PWR fuel rods is typically localized in the lowermost regions of fuel within the flow recovery regions just beyond the bottom nozzle where the flows are most turbulent and cross-flow conditions are most likely to exist. The fretting behavior is entirely independent of fuel assembly length since the key observed parameters governing fretting resistance are associated with rod support characteristics, cross-flow velocities, span distance, and materials.

The U.S. EPR design does not introduce additional features or characteristics other than overall length to the evaluation. Span lengths are no greater than those used on existing 12 ft designs.

The 1000 hour HERMES-P flow testing was conducted under extreme and very conservative tests conditions. These tests were not intended to provide the sole basis for licensing, but are presented only to characterize the fretting performance in terms of the extreme conditions needed to produce significant discriminating levels of fretting associated with grid features and test conditions. The tests used varying levels of grid contact ranging from very slight interference to open gap clearances. The tests were performed at operating temperature using a full-scale fuel assembly prototype with characteristics representative of a U.S. EPR fuel assembly. The testing incorporated a large cross-flow injection port at the bottom span so that the total flow exiting the fuel assembly is greater than the flow entering the bottom nozzle.

Supplementary tests to establish FIV performance of the U.S. EPR fuel assembly have been conducted with EPR mock-up fuel using the PETER Loop/Autoclave flow test method. This testing is applicable to the U.S. EPR due to the close mechanical similarity to the prototype fuel assembly that was tested. The PETER Loop testing measured fuel rod and fuel assembly flow-induced vibration behavior for a full-scale fuel assembly prototype during parametric in-reactor flow conditions. The PETER Loop testing also determines the most FIV-limiting span and fuel rod position for subsequent investigations of endurance wear testing within the Autoclave test facility. Vibration amplitudes for the fuel assemblies were very low over a 1 to 50 Hz frequency range. No abnormal flow rate dependencies were observed for the fuel assembly vibration amplitudes.

The second part of the PETER Loop/Autoclave testing consisted of additional endurance fretting wear tests on a single fuel rod in the Autoclave test facility. The dynamic input from the PETER Loop flow test with added conservatism, including twice the normal cross-flow was used for the single rod fretting test. The rod was subjected to precisely replicated mechanical support conditions and mechanical

excitations representing worst-case rod support, conditions including EOL plus open gap rod-to-grid interface conditions.

Fretting marks were not found on the EOL Autoclave tested fuel rod specimens with flow exposures up to 1000 hours. This favorable fretting behavior is attributed to the line-type contact and higher inherent damping of the HTP grid design. Therefore, the U.S. EPR fuel assembly resists fretting for the excitations that could be experienced in a U.S. EPR.

The test results confirm that due to cross-flow within the flow recovery regions near the bottom of the assemblies, the bottom span experiences the most turbulent flow regimes. Very conservative and bounding rod motions were imposed for significant duration during the wear tests and no excessive wear was produced. The applicability of these test results and conclusions to the U.S. EPR is supported by extensive operating experience.

Operating experience also supports the out-of-core test results as detailed in Reference 1. A large number of fuel assemblies with HTP spacers have been in operation in many nuclear power plants worldwide. The population of these fuel assemblies includes significant burnup levels in excess of 40 GWD/MTU, with a maximum assembly burnup of 70 GWD/MTU having been achieved. Within the population of HTP fuel assemblies, only a very small number have ever experienced failure due to grid-to-rod fretting. There have been no grid-to-rod fretting failures in fuel assemblies that have HTP type grids at end grid locations.

In summary, the U.S. EPR fuel rod fretting and wear performance is acceptable based on relevant incore experience and extensive and conservative out-of-core testing.

4.2.3.6 Reactivity Control, Neutron Source, and Thimble Plug Assemblies

4.2.3.6.1 Internal Pressure and Cladding Stresses

The U.S. EPR RCCA control rod internal pin pressure analysis shows that absorber internal pin pressure remains below the system pressure of 2250 psig under normal operations and AOOs. The control rod internal pressure was calculated using a conservative model and bounding input and assumptions. The AIC alloy does not generate gases due to radiation exposure. Since there is no B_4C used in the U.S. EPR control rod, there are no sources of gas generation that could contribute to internal pressurization.

Control rod internal pressure during accident (LOCA) conditions has also been evaluated and the maximum internal rod pressure has been calculated to assess the effect on the cladding hoop stresses. The analysis shows that hoop stresses remain below the burst strength for the 316L stainless steel cladding under postulated accident conditions (see Chapter 15).

Cladding stresses have been determined considering the loading conditions covering normal operation, AOOs, and PAs. The stress limits of Subsection NG of the ASME Code, Section III, (Reference 4) have been used as guidance for conditions of normal operations and for AOOs, and for the hoop burst strength for PAs. In all cases the cladding stresses remain within acceptable stress limits.

RCCA cladding creep collapse has been evaluated using the same methods as that used for fuel rods. Results show that the RCCA cladding does not collapse within the 15 year design life. The collapse analysis is based on an internal control rod prepressure of 220 psig.

Primary and secondary neutron source rods have also been analyzed for internal rod pressure. For both rod types, internal pressure remains well below the system pressure of 2250 psig. The analysis accounts for internal gas generation from the Sb-Be secondary source material. The primary source materials do not generate gases due to irradiation. However, the alumina spacers within the primary source rods swell during irradiation, and the increased pressure from the reduction in the internal void volume is taken into account.

Neutron source rod cladding stresses have also been calculated. Cladding stresses are shown to remain below the stress limits, using the same ASME strength limit definitions for control rod cladding.

4.2.3.6.2 RCCA and SCCA Spider Structural Analysis

Structural analysis of the RCCA spider evaluated the effects of loading from CRDM operational stepping, RCCA reactor trip, stuck rod, fatigue, and shipping and handling. As stated in Section 4.2.1.6.3, stress limits are derived from Reference 4. The components of the spider assembly that were evaluated include the vanes, hub, spring, retaining ring, retainer bolt (shank and threaded area), and brazed joints. The threaded regions of the vanes and fingers where the RCCA rods connect with the spider were also analyzed. In all cases the stresses are shown to be below the design limits, including fatigue limits.

An important design basis for the RCCA requires the RCCA spider spring to absorb the kinetic energy of the CRDM driveline (drive rod plus RCCA) following reactor trip. Two conditions must be met during the trip event:

1. The spring is not compressed to a solid height.
2. The full retainer stroke does not exceed the maximum allowed limit of 1.075 in (Table 4.2-4).

The analysis shows that both conditions are met, thereby avoiding hard contact between the bottom of the spider hub and the top surface of the fuel assembly.

The SCCA spider, although similar in configuration to the RCCA spider, is a stationary component, held in place between the upper core plate and the top surface of the fuel assembly top nozzle grillage. The stress analysis for the spider hub, vanes, and spring (including fatigue loads on the spring) shows positive margin to the applicable design strength limits.

Interface analysis of the SCCA spider shows that the spider hub does not interfere between the fuel assembly top nozzle and upper core plate in the case of solid contact between these components (i.e., a fuel assembly-to-upper core plate gap of zero).

Irradiation induced relaxation of the SCCA Alloy 718 spring—along with hydraulic flow, buoyancy loads, and component mass—was taken into account in determining the design life of the spring to verify that hold down of the SCCA is maintained for the TPA and both types of source assemblies. The design life for the TPA spider spring was shown to exceed the life of the plant, while the design life for the source assembly spring exceeds the minimum design life for the source assemblies.

4.2.3.6.3 Thermal Stability of the Absorber Material

The AIC absorber alloy is currently used in U.S. PWRs. AIC exhibits slow, time-dependent thermal creep at reactor operating temperature, and this thermal behavior is considered in assessing U.S. EPR RCCA rod performance. Axial thermal creep of the AIC in response to loads imposed by the absorber mass and plenum spring contributes to a slow expansion of the AIC diameter at the absorber bottom end. The eventual contact between absorber and cladding results in compressive hoop stresses in the AIC that cause significant thermal creep at the inner surface of the absorber, thereby relieving the interference stresses between the cladding and absorber.

The U.S. EPR RCCA control rod thermal analysis shows that absorber and cladding temperatures remain below material melt temperatures, using bounding assumptions and analysis input. The control rod internal pressure was calculated using a conservative model and was shown to be below system pressure. The AIC alloy does not generate gases from radiation exposure, and therefore does not contribute to internal rod pressure.

Phase changes of the AIC material resulting from irradiation are taken into account with the radiation swelling model.

4.2.3.6.4 Irradiation Stability of the Absorber Material

The control rod absorber AIC alloy does not generate gases due to irradiation, and therefore does not contribute to internal rod pressure. However, irradiation swelling of the absorber material occurs and is accounted for in the lower section of the absorber where the thermal neutron flux exists. AIC irradiation swelling is modeled based on in-reactor data acquired in hot cell examinations.

4.2.3.6.5 Potential for Chemical Interaction

Chemical interaction between the RCCA materials and neutron sources are limited and are considered insignificant in terms of degradation mechanisms of the structural and absorber materials. The materials comprising the control components are either low-carbon 300-series austenitic stainless steels (304L, 308L, 316L), AISI 630 grade stainless steel, or Alloy 718, all of which are resistant to corrosion degradation from exposure to PWR coolant. Section 5.2.3.2, provides information on those aspects of the reactor coolant chemistry that provide corrosion protection for stainless steels and nickel alloys. A comprehensive review of the U.S. EPR reactor coolant environment and the potential effect on corrosion of these materials is available.

The control rod absorber is encapsulated in a 316L stainless steel tube that is welded at both ends. This protects the AIC from the coolant, however the AIC alloy is not susceptible to significant corrosion rates should the cladding barrier be breached, and loss of absorber material to the reactor coolant is not a likely event in this case.

4.2.4 Testing and Inspection Plan

The testing and inspection plans for fuel rods, fuel assemblies, and control components are expected to follow the same rigorous methods and criteria as components currently manufactured and licensed for use in PWR units in the U.S. The current fuel fabrication plants operated by the Fuel Sector of AREVA NP are expected to be utilized for fabrication of the U.S. EPR fuel rods and control components. The current quality assurance program approved per 10 CFR 50, Appendix B is used for the U.S. EPR fuel rods and control components.

4.2.4.1 Operating Experience

The AREVA NP fuel product lines establish the operating experience basis for the overall U.S. EPR fuel assembly construction, including the MONOBLOC™ guide tubes with QD connections, HTP and HMP spacer grids, the welded cage (skeleton), and the FUELGUARD™ bottom nozzle. The AREVA M5™ fuel products establish the global and domestic operating experience basis for the M5™ fuel rod cladding and guide tube implementation, including the 17x17 Advanced Mark-BW fuel design from which the low pressure drop top nozzle is derived. AREVA NP is also the principal supplier of 14 ft fuel assemblies and has international experience in all fuel design features that are pertinent to the U.S. EPR design.

A discussion of the operational behavior and reliability of other AREVA NP-designed fuel assemblies that is pertinent to the design of the U.S. EPR fuel assembly is provided in Reference 1.

4.2.4.1.1 HTP Grid Experience

HTP is primarily the designation for a special type of spacer. However, it is also used to denote a fuel assembly design, such as the U.S. EPR design, in which this type of spacer is a major component. Fuel assemblies equipped with traditional spacers employ springs and dimples to support each fuel rod in its spacer cell, and have mixing vanes along the top edges of the spacer strips that significantly enhance thermal-hydraulic performance. In contrast, the HTP spacer is a different yet proven concept in spacer design for PWR fuel. The HTP spacer features strip doublets that are shaped such that they not only serve as spring elements to firmly hold the fuel rods in radial alignment, but also produce curved internal flow channels to achieve the desired thermal-hydraulic performance. Their first use was in a U.S. plant in 1988, and the HTP design now has 18 years of global operational experience.

As of December 2006, 7894 HTP fuel assemblies have been irradiated in 41 reactors internationally, including 2995 assemblies in twelve U.S. plants. This experience spans the entire range of fuel rod arrays from 14x14 to 18x18, as well as reactors supplied by vendors such as CE, Framatome, Westinghouse, Siemens, and B&W (since 2003). Close to one-half of the HTP assemblies (3816) have been loaded into 12 ft Framatome and Westinghouse plants with a 17x17 array. A significant portion of the deployed HTP assemblies have been loaded into CE- and Westinghouse-designed plants, totaling 7.5–9.5 percent for the 14x14 or 15x15 arrays, respectively. The operational experience with HTP assemblies in Siemens designed plants continues to increase. To date, a total of 1120 HTP fuel assemblies have been inserted into 14 Siemens designed plants, including plants with 15x15, 16x16 and 18x18 arrays.

Fuel assemblies with HTP spacers made of Alloy 718 at the lowermost position were first inserted into two German plants in 1992. These Alloy 718 spacers had the same curved flow channels as the zircaloy HTP spacers in the active region of the fuel. The initial insertion of the current version of Alloy 718 spacers with straight flow channels, designated HMP, occurred in 1988. Today, a large operating experience base with HTP fuel featuring the HMP spacer is available. Altogether, 2597 of these HTP fuel assemblies have been loaded into 26 plants worldwide. A maximum assembly burnup of 70 GWD/MTU has been achieved.

The selection of M5™ strip material for construction of U.S. EPR HTP intermediate spacers is based on the favorable operating experience of M5™ alloy application for fuel rod cladding and guide tubes. The benefits of reduced corrosion (i.e., lower oxide layer formation rate) and hydrogen pickup results in greater strength at higher burnups, from a spacer that offers a lower loss of structural strip thickness and additional margins against loss of ductility.

The application of M5™ for intermediate spacer grids in the U.S. EPR is consistent with the intention of AREVA NP to maximize the use of M5™ within the entire

product line of PWR fuels in the future. In 2004, the first HTP lead assemblies equipped with M5™ spacers and M5™ MONOBLOC™ guide tubes were inserted into two German plants. In 2005, two reloads with M5™ HTP 15x15 spacers were placed into two U.S. plants, and two additional reloads were installed in 2006 and 2007. In 2006, one reload of M5™ HTP 14x14 fuel assemblies was implemented in the U.S. and four M5™ HTP 17x17 lead assemblies were installed in a Swedish plant.

Since 1991, HTP fuel assemblies with Zircaloy-4 spacers at the top end grid position have been inserted into U.S. plants. As of December 2006, a total of 3515 HTP fuel assemblies equipped with an upper HTP spacer made of zirconium alloy have been irradiated in 29 plants worldwide.

HTP fuel assemblies equipped with M5™ clad rods were first inserted into four plants in 2003, including four lead test assemblies in both a South American and U.S. plant, a reload consisting of 36 16x16 assemblies in a German plant, and one reload with 85 15x15 assemblies in a U.S. plant. By December 2006, 1171 HTP fuel assemblies with M5™ cladding have been irradiated in 20 plants in Germany, the Netherlands, Sweden, Switzerland, South America, and the U.S. The operational experience of the combination HTP fuel assembly and M5™ cladding includes arrays from 14x14 up to 18x18. To date, a maximum assembly average burnup of 51 GWD/MTU has been achieved.

4.2.4.1.2 M5™ Experience

M5™ is an advanced zirconium alloy developed and implemented by AREVA NP to improve corrosion resistance, reduce hydrogen uptake, and reduce irradiation growth. In 1999, the NRC approved M5™ for domestic use (Reference 2). To date, 33 reloads in 15 different U.S. reactors have used the M5™ alloy in more than 2300 fuel assemblies. Globally, over 1.5 million M5™ fuel rods have operated in approximately 6500 fuel assemblies within 57 reactors, and more than 3000 fuel assemblies with both M5™ fuel rods and guide tubes have operated in 37 reactors. Reference 1 provides additional information on the global scale of M5™ fuel rod usage and the international distribution of these fuel assemblies, including the global usage of M5™ material for cladding, guide tubes, and spacer grids within various types of fuel assemblies.

4.2.4.1.3 14 Foot Experience

AREVA also has extensive experience in the design and supply of 14 ft long fuel assemblies, mainly for two designs used in the European N4 and 1300MW reactors, four and 20 plants respectively. The first batch of 14 ft fuel was installed in 1983 and to date (mid-2007) AREVA NP has supplied over 2,000 of these fuel assemblies.

4.2.4.1.4 RCCAs

Worldwide, more than 4,600 ion-nitrided HARMONI™ RCCAs have been delivered to operating reactors in nine countries, including 572 ion-nitrided RCCAs at 11 PWRs in the U.S. The first U.S. HARMONI™ RCCAs were delivered in mid-1995.

4.2.4.2 Fuel Assembly Prototype Testing

A comprehensive test program was conducted to characterize the performance of the U.S. EPR fuel assembly design. Testing was conducted on full-sized prototype fuel assemblies and on various assembly components. The full-size, 14 ft prototype fuel assemblies were used for structural, mechanical, and thermal-hydraulic testing. The prototype fuel assembly structural and mechanical tests included static axial tension and compression tests to determine fuel assembly axial stiffness; static lateral bending to determine lateral stiffness; fuel assembly shaker tests to determine natural frequencies and mode shapes; lateral pluck tests with and without spacer grid impact to determine fuel assembly damping; and vertical drop tests from various heights.

The prototype fuel assembly thermal-hydraulic test scope included assembly pressure drop tests, life and wear testing consisting of a 1000 hour endurance test in the HERMES-P loop, and flow-induced vibration testing. In addition, RCCA SCRAM tests (i.e., trip times) and stroking wear tests were performed in the KOPRA test loop (Reference 1).

These tests, described in detail in Reference 1, were conducted in accordance with approved test plans, at QA approved AREVA NP test facilities. The test results were used in benchmarking analytical models for the U.S. EPR fuel assembly design evaluation addressed in Section 4.2.3.5 above.

4.2.4.2.1 Shaker Testing

The prototype fuel assembly (OL3) was supported by mock core plates with guide pins to simulate the end conditions in the reactor. The frequency and damping values and the mode shapes for the first five modes of vibration of the fuel assembly were measured. An electrodynamic shaker was used to excite the fuel assembly near the midplane at various frequencies and amplitudes as the responses of the fuel assembly nozzles and spacer grids were measured and recorded. These displacement time histories were analyzed to determine the dynamic characteristics of the fuel assembly.

4.2.4.2.2 Lateral Pluck Testing

A fuel assembly pluck test was performed on the prototype fuel assembly in air and in water at room temperature to obtain fundamental natural frequency and damping values at various amplitudes. The pluck test was conducted by measuring and recording the displacement of selected spacer grids as the fuel assembly was deflected

laterally at the midplane and quickly released. The results were consistent with the shaker test results for the first mode. Submersion of the fuel assembly in water reduced the fundamental frequency but had no measurable effect on the damping.

4.2.4.2.3 Static Stiffness Testing

Forces versus deflection tests were conducted to determine the axial and lateral stiffness of the prototype fuel assembly. In an axial stiffness test, the fuel assembly was compressed along its longitudinal axis by an application of forces at the nozzles. The lateral stiffness test consisted of loading the fuel assembly laterally at the two center spacer grids.

4.2.4.2.4 Fuel Assembly Drop Testing

Fuel assembly drop tests were performed on a prototype fuel assembly to obtain impact loads against which the vertical analytical model was benchmarked. The fuel assembly was dropped from various heights against an unyielding surface and the impact loads were measured and recorded. The effects of multiple drops in succession were accounted for in the model benchmark, and a suitable correlation to the test results were obtained.

4.2.4.2.5 Fuel Hydraulic Flow Testing

Full-scale flow testing on a full-scale prototype fuel assembly was performed in the HERMES-P flow loop test facility. These flow loop tests were used to establish flow loss coefficients and other related flow characterization parameters for inputs to the LYNXT thermal hydraulic flow analysis computer code. The LYNXT code was approved for use in evaluating fuel assembly designs in LYNXT Topical Report (Reference 16). LYNXT was used to determine the flow lift forces on the fuel assembly as a part of the evaluation of fuel assembly lift-off resistance.

The prototype fuel assembly tests also were used to evaluate the fretting and wear performance at the grid-to-rod interfaces. Fretting resistance was also demonstrated with combined out-of-core testing performed in the PETER Loop and Autoclave test facilities. The PETER Loop test facility provided short-term measurement of FIV parameters on a full-scale fuel assembly at temperature and pressure. From the rod and grid vibration parameters, such as amplitude and frequency, the worst-case rod and axial region of fuel assembly flow were determined. These bounding vibration conditions were then replicated in the Autoclave test apparatus involving an individual rod and limited axial span, but with extended time spans of up to 1000 hours to enable testing on a bounding and worst-case rod-to-grid interface.

4.2.4.2.6 CRDM Driveline and RCCA Testing

The U.S. EPR RCCA has been performance tested in a full-scale test loop, which includes the CRDM, drive rod, RCCA, and receiving fuel assembly cage mockup. The test program measures various parameters relating to RCCA drop kinetics, i.e., various pressure drop conditions and driveline drop time. The program includes an endurance phase that evaluates mechanical wear of components such as the driverod, CRDM latching mechanism, and control rod guide assembly. The test program is designed to demonstrate proper equipment operation of the CRDM and driveline in response to stepping and simulated rod drop events. The performance testing phase is complete, having encompassed three million steps. However, additional steps and driveline trips are planned to validate the endurance capability of the CRDM and driveline.

Of particular interest to the fuel assembly guide thimble and RCCA design is the measured drop time data used to benchmark the performance code that is used to calculate and predict the drop kinetics of the U.S. EPR driveline under various conditions, including maximum and minimum rod drop conditions. The maximum rod drop time was determined to be less than the specification limit.

The minimum drop time relates to the maximum impact velocity of the RCCA with the fuel assembly top nozzle, and is used to validate the structural integrity of the RCCA spider spring. The results of that analysis shows that the spring performs as expected and a hard mechanical shock between RCCA spider hub and fuel assembly top nozzle does not occur.

Stepping acceleration and deceleration loads are also measured in the test loop using instrumentation directly applied to the drive rod. Stepping loads specific to the RCCA are determined and used in the mechanical analysis of the RCCA spider and rods.

The final results of the testing will provide the confirmation of the mechanical endurance capability of the CRDM mechanisms, and also confirm that drop times are not adversely affected following the endurance phase of the test program.

4.2.4.3 Fuel Assembly Component Testing

In addition to full-scale prototype testing, various components were also characterized by testing. Static compression tests were performed on the hold-down springs and clamp screw. The spacer grid design was subjected to static buckling and dynamic crush tests. The strength of the component connections and bottom nozzle were also tested. These test results were incorporated into various analytical models used to verify the U.S. EPR design.

4.2.4.3.1 Strength Test of Upper Guide Tube Connection

Hot compression tests of the upper guide tube QD connection were conducted to determine the static strength of this connection. The tests determined that the guide tubes fail plastically without failure of the spot welds used to attach the QD fittings to the end of each guide tube. Therefore, the test shows that the mechanical strength of the QD connector is limited by the performance of the guide tube and not by the welded connection between the sleeve and guide tube.

4.2.4.3.2 Spacer Grid Testing

The mechanical design bases for the U.S. EPR spacer grids were confirmed through a series of structural tests on prototype grids. The testing, summarized below, found that the grids provide the necessary design margins:

- Dynamic Impact: The dynamic characteristics at BOL hot conditions (impact force, impact duration, pre- and post-impact velocity, grid permanent deformation, dynamic stiffness, and damping) were used as input properties for the analytical models of the fuel assembly, to establish allowable impact loads, and to characterize the plastic deformation of the grids.

- Static Crush: The static characteristics (static stiffness and elastic load limit) were used to establish allowable grid clamping loads during shipping.

- Slip Load: The forces required to slip the grid relative to the fuel rods were measured at BOL conditions for both M5™ HTP and Alloy 718 HMP grids. Grid slip load measurements are provided in the Fuel Assembly Mechanical Design Topical Report (Reference 1).

- Corner Hang-up (spacer grid): The U.S. EPR HTP grid corners have been designed (through the use of lead-in surfaces) to minimize the potential for grid hang-up. Previous testing on 15x15 M5™ HTP grids fuel assemblies showed that M5™ grids have corner strength much greater than the maximum pull and push handling load criteria in Reference 1. The test results were conservative because the grid corners are designed with a lead-in to force the grids to lead off laterally and reduce the interference. The testing method allowed no lead-off.

  In addition, these spacer grid tests determined the failure mode of the corner cell (simulating grid hang-up) was through weld fracture with very little outer strip and corner deformation. Given the similarities in the design, these test results are considered applicable for U.S. EPR design certification purposes.

4.2.4.3.3 Strength Test of Bottom Nozzle

Strength testing of the bottom nozzle was performed to establish the axial load limit criteria for evaluation. A prototype bottom nozzle was tested at room temperature in static axial compression by 24 springs on the guide tube positions. The spring stiffness was set to be equal to the guide tubes stiffness in order to simulate the real load

distribution of the guide tubes. The test piece and the bottom nozzle for the U.S. EPR design are identical except that the test piece has a central instrument tube position that is not present in the U.S. EPR design. The influence of this difference on the strength behavior can be neglected. A maximum room temperature test load was demonstrated without collapse of the structure. This tested maximum load was used to demonstrate the structural adequacy in the design evaluation by comparison with the normal operating and faulted loads, as discussed in Section 4.2.3.5.1.

4.2.4.3.4 Hold-down Spring Characteristic Tests

Static force deflection tests were performed on prototype sets of the U.S. EPR fuel assembly five-leaf hold-down springs at room temperature to obtain the force and deflection characteristics of the spring. The force and deflection characteristics were used in the normal operating analysis to determine fuel assembly hold-down forces. The hold-down spring rate was determined from the test data and used in the analytical model of the fuel assembly.

4.2.4.4 Testing and Inspection of New Fuel

New fuel and control components and assemblies are manufactured and inspected in accordance with the AREVA NP Quality Assurance program as described in Chapter 17. In general, components and assemblies are tested and inspected to verify compliance to all design drawing and specification requirements. Quality Control procedures are prepared and used for all inspection operations. Quality Control maintains a gauge control system for tooling, gauges, templates, and other equipment used to perform inspections. Inspection plans range from 100 percent inspection plans to statistical process control procedures, which require either upper and lower tolerance limits, upper and lower confidence limits, or other statistically-based (attribute or variable) sampling plans.

The Quality Assurance program requires audits of suppliers and internal audits of AREVA NP manufacturing and inspection operations.

Materials are procured from approved suppliers using approved material specifications, which may include industry-approved standards (such as ASME and ASTM materials specifications) and AREVA NP internal specifications. Certified material test reports are required for all safety-related materials and are reviewed for conformance to the specification requirements.

Depending on the particular design requirement to be verified, non-destructive examinations (dimensional, visual, radiographic, ultrasonic, and eddy current inspection) and destructive examinations (chemical composition and metallographic sectioning) may be employed for both in-process inspections, or in support of qualifications.

The AREVA NP manufacturing operations require stringent adherence to cleanliness controls for all components and assemblies, and cleaning qualifications serve as the primary means of demonstrating that the cleanliness criteria have been met. The cleanliness program also includes controls for all expendable and consumable materials that come in contact with core components.

Fuel pellets are extensively tested and inspected, including: dimensional inspections, visual examinations to check for surface contamination and surface defects, destructive examinations for microstructure (grain size and pore size distribution), resinter densification, chemical composition, and impurity checks (including hydrogen determination and isotopic content). Additional examinations and tests are required for qualifications.

Fuel rod cladding tubes are inspected for external and internal defects by approved non-destructive methods. Ultrasonic methods are used for dimensional measurements. Fuel rod welds are tested by both destructive and non-destructive means, are leak tested using helium detection equipment, and are then gamma-scanned to verify the integrity and position of the internal components and the absence of unacceptable pellet gaps. Automated computer equipment is used to maintain traceability of pellets, cladding, and fuel rods on a lot basis. Traceability of other components is accomplished with assembly identification and standard tagging methods.

Fuel assemblies must undergo inspections for length, bow, twist, dimensional envelope, and water channel criteria. Visual examinations are performed as a final check on cleanliness control.

4.2.4.5 On-Line Fuel System Monitoring

Section 9.3.2 describes the methods and systems for on-line monitoring to detect failed fuel.

4.2.4.6 Postirradiation Surveillance

AREVA NP maintains a multifaceted postirradiation examination (PIE) surveillance program that is designed to maintain compliance with regulatory requirements, maintain awareness of emerging nuclear industry and regulatory issues, support design optimization and product development, and address operational issues. The program is committed to a culture of safety, quality, continuous improvement, and zero tolerance for failure. PIE activities include both poolside and hot cell examination campaigns, both of which may include inspections and examinations for cladding oxide (corrosion) thickness, hydrogen content, crud deposition, irradiation growth of fuel rods and assemblies, shoulder gap measurements, fuel rod fretting, damage incurred from handling or debris, and general dimensional attributes. The AREVA NP PIE program, compiled into a four-year rolling schedule of PIE campaigns at various

nuclear power plants and laboratories, represents part of a comprehensive fuel reliability program. The AREVA NP fuel reliability program works with the Institute of Nuclear Power Operations and the Electric Power Research Institute to develop strategies for PIE exams that will reduce or eliminate fuel damage and fuel rod failures. Postirradiation examinations also apply to control components (RCCAs) to monitor the presence and extent of control rod cladding damage (fretting and wear) and swelling of absorber materials.

4.2.5 References

1. ANP-10285P, Revision 0, "U.S. EPR Fuel Assembly Mechanical Design Topical Report," AREVA NP Inc., October 2007.

2. BAW-10227P-A, Revision 1, "Evaluation of Advanced Cladding and Structural Material (M5™) in PWR Reactor Fuel," Framatome Cogema Fuels, June 2003.

3. ANP-10263P-A, Revision 1, "Codes and Methods Applicability Report for the U.S. EPR," AREVA NP Inc., November 2007.

4. ASME Boiler and Pressure Vessel Code, Section III, "Rules for Construction of Nuclear Facility Components," The American Society of Mechanical Engineers, 2004.

5. BAW-10186P-A, Revision 2, "Extended Burnup Evaluation," Framatome Cogema Fuels, January 2004.

6. BAW-10231P-A, Revision 1, "COPERNIC Fuel Rod Design Computer Code," FRAMATOME ANP, September 2004.

7. BAW-10183P-A, "Fuel Rod Gas Pressure Criterion," B&W Fuel Company, July 1995.

8. BAW-10133PA-01, Addendum 1 & 2, "Mark-C Fuel Assembly LOCA-Seismic Analysis," Framatome Cogema Fuels, October 2000.

9. BAW-10240P-A, Revision 0, "Incorporation of M5™ Properties in Framatome ANP Approved Methods," Framatome ANP, Inc., August 2004.

10. ASME Boiler and Pressure Vessel Code, Section II, "Materials," The American Society of Mechanical Engineers, 2004.

11. NUREG-0800, Revision 3, "Standard Review Plan for the Review of Safety Analysis Reports for Nuclear Power Plants," U.S. Nuclear Regulatory Commission, March 2007.

12. W.J. O'Donnell and B.F. Langer, "Fatigue Design Basis for Zircaloy Components," Nuclear Science and Engineering, Volume 20, pp. 1-12, April 1, 1964.

13. ANF-89-060(P)-A, Supplement 1, "Generic Mechanical Design Report High Thermal Performance Spacer and Intermediate Flow Mixer," Siemens Power Corporation, February 1991.

14. BAW-10172P-A, Revision 0, "Mark-BW Mechanical Design Report," Babcock & Wilcox, December 1989.

15. BAW-10239P-A, Revision 0, "Advanced Mark-BW Fuel Assembly Mechanical Design Topical Report," Framatome ANP, Inc., October 2004.

16. BAW-10156-A, Revision 1, "LYNXT: Core Transient Thermal-Hydraulic Program," B&W Fuel Company, August 1993.

17. BAW-10147P-A, Revision 1, "Fuel Rod Bowing in Babcock & Wilcox Fuel Designs," Babcock & Wilcox, June 1983.

Table 4.2-1—U.S. EPR Fuel Assembly Design Summary

Parameter	Value or Description
Fuel Assembly Parameters	
Number of fuel rods per assembly	265
Number of guide tubes per assembly	24
Number of intermediate grids per assembly	8
Number of end grids per assembly	2
Fuel assembly envelope	8.426 in
Fuel rod pitch	0.496 in
Fuel Rod Parameters	
Cladding material	M5
Cladding outside diameter	0.3740 in
Cladding inside diameter	0.3291 in
Fuel column length	165.354 in
Overall fuel rod length	179.134 in
UO_2 Pellet Parameters	
Outside diameter	0.3225 in
Length	0.531 in
Fissile enrichment	≤ 4.95 wt% U-235
UO_2-Gadolinia Pellet Parameters	
Outside diameter	0.3225 in
Length	0.531 in

Table 4.2-2—Fuel Assembly Materials

Component	Material
Top nozzle	AISI 304 L stainless steel
Hold down spring leaf	Nickel Alloy 718
Hold down spring screw	Nickel Alloy 718
Anti-debris bottom nozzle	AISI 304 L stainless steel
Guide thimble, guide thimble plugs, and QD sleeves	M5™
Top connection (quick disconnect)	M5™ and Alloy 718
Bottom socket head screw	AISI 316 L stainless steel
HMP grid	Nickel Alloy 718
HTP grid	M5™
Fuel rod cladding	M5™
Fuel rod end plugs	M5™
Fuel rod plenum springs	AISI 302 stainless steel
Fuel rod support tube	321 stainless steel
Fuel pellets	UO_2 and $UO_2 + Gd_2O_3$

Table 4.2-3—RCCA, Source Assembly, and TPA Component Materials

Component	Structural Material and Condition	UNS Designation
Spider, tension bolt	AISI 304 L (quench annealed)	S30403
Rod end plugs, pins, thimble plugs, bullet head nuts	AISI 308 L	S30803
Tubular cladding	Seamless and cold-drawn AISI 316 L (ion-nitrided outer surface for RCCA cladding only)	S31603
Retaining ring	AISI 630 (17-4 PH stainless steel, SA-564, condition H1100)	S17400
Spider spring	Cold drawn, precipitation hardened Alloy 718	N07718
Control rod plenum spring	Cold drawn, precipitation hardened Alloy X-750	N07750
AIC absorber material	80% Ag - 15% In - 5% Cd	NA
Primary neutron source	Cf-252 + stainless steel	NA
Secondary neutron source	Cold pressed antimony-beryllium pellet	NA

Table 4.2-4—RCCA Characteristics and Design Parameters
Sheet 1 of 2

Component / Feature	Nominal Value
RCCA General Characteristics	
RCCA total mass	136.3 lb_m
RCCA total height	185.726 in
Spider height (top of hub to lower end of finger)	8.994 in
Number of rods per RCCA	24
Distance between end of retaining ring and rod lower end plug	176.850 in
RCCA Spider	
Mass	7.660 lb_m
Hub outer diameter	1.838 in
Hub length	7.814 in
Coupling hub depth (peripheral)	2.140 in
Coupling groove minimum inner diameter	1.338 in
Hub counter-bore (spring cavity) length	5.299 in
Hub counter-bore (spring cavity) diameter	1.490 in
Number of vanes	16
Finger diameter	0.361 in
Retainer ring travel (max)	1.075 in
RCCA Spring	
Wire diameter	0.302 in
External coil diameter	1.435 in
Number of coils (total/active)	12.5/10.5
RCCA Rod	
Mass (one rod with absorber)	5.36 lb_m
Mass (24 rods with absorber)	128.6 lb_m
Overall rod length	178.331 in
Functional rod length	177.972 in
Maximum local rod diameter (weld)	0.386 in
Lower end plug diameter	0.381 in
Cladding outer diameter	0.381 in
Cladding inner diameter	0.3440 in
AIC bar overall length	166.929 in
AIC bar upper region diameter	0.341 in

Table 4.2-4—RCCA Characteristics and Design Parameters
Sheet 2 of 2

Component / Feature	Nominal Value
AIC bar lower region diameter	0.336 in
AIC bar low region (reduced diameter) length	16.0 in
Minimum cladding wall thickness	0.0169 in
AIC inner hole diameter	0.174 in
Initial rod pre-pressure	220 psig
RCCA Rod Plenum Spring	
Wire diameter	0.058 in
External coil diameter	0.334 in
Number coils (active/total)	81/83

Table 4.2-5—Control Component Mechanical Strength

Material	Minimum Value (ksi)					
	Nickel Alloy 718	AISI 304L	AISI 308L	AISI 316L	AISI 316L ion-nitrided	AISI 630
Component	spider spring	spider, tension bolt	rod end plugs, pins, nuts	source cladding	AIC absorber cladding	spring retainer
0.2% Y.S., cold	210.3	30.0	45.7	71. 1	70.5	114.8
0.2% Y.S., hot	190.0	18.1	37.0	60.9	53.4	92.8
UTS, cold	229.1	75.0	90.6	100.1	100.1	140.0
UTS, hot	206.6	63.5	77.6	84.8	87.7	131.4

Table 4.2-6—SCCA Characteristics and Design Parameters
Sheet 1 of 3

Component / Feature	Nominal Value
SCCA Spider Assembly	
Spider assembly length (top of hub to bottom of retaining ring)	8.071 in
Retaining ring travel	1.969 in
Spider finger elevation from ring lower face (4 “central” fingers)	6.142 in
Spider finger elevation from ring lower face (other fingers)	5.315 in
SCCA Spider	
Maximum hub outer diameter in the vanes region	1.890 in
Number of vanes	16
Number of guide rings	
Type 1 TPAs and primary and secondary source assemblies	0
Type 2 TPAs	1
Type 3 TPAs	2
Finger diameter, normal	0.358 in
Finger diameter, reinforced	0.431 in
Vane thickness	0.140 in
Minimum vane height	1.811 in
Distance between top of extended vanes and lower hub end	3.543 in
Spider Hub Dimensions	
Total length	6.102 in
Coupling cavity length	2.140 in
Groove minimum inner diameter	1.338 in
Coupling cavity/spring cavity wall thickness	0.104 in
Length of the spring in the cavity without external compression	3.622 in
"Circular stop" thickness	0.118 in
Spring cavity internal diameter	1.433 in
External diameter	1.839 in

Table 4.2-6—SCCA Characteristics and Design Parameters
Sheet 2 of 3

Component / Feature	Nominal Value
Spider Ring Dimensions	
Instrumentation Ring	
Height	0.472 in
Internal diameter	0.472 in
External diameter	0.669 in
Retaining Ring	
"Circular stop" thickness	0.118 in
Total Length	2.205 in
Spider Spring Dimensions	
Wire diameter	0.126 in
Ext. coil diameter	1.386 in
Free length	6.043 in
Max. solid length	1.555 in
Number of working coils	10.5
Thimble Plug Assemblies	
Type 1 Assemblies	
Quantity (initial quantity/ultimate quantity) Note: initial quantity is plant specific	≈106 / 112
Number of plugs	20 short; 4 long
Type 2 Assemblies (instrumented)	
Quantity	28
Number of plugs	19 short; 4 long
Type 3 Assemblies (instrumented)	
Quantity	12
Number of plugs	18 short; 4 long
TPA total height	14.010 in
Distance between end of retaining ring and thimble plug lower end	5.939 in
Overall thimble plug length (short)	11.293 in

Table 4.2-6—SCCA Characteristics and Design Parameters
Sheet 3 of 3

Component / Feature	Nominal Value
Overall thimble plug length (long)	12.120 in
Rod diameter (part in the fuel assembly guide tubes)	0.422 in

Table 4.2-7—Rod Parameters for Primary and Secondary Source Assemblies

Feature	Nominal Value (cold)	
	Primary Source Rod	Secondary Source Rod
Number of rods in assembly	1	20 short, 4 long
Distance between end of retaining ring and rod lower end plug	155.547 in	155.485 in
Overall rod length (primary or secondary long)	160.902 in	161.667 in
Overall rod length (secondary short)	NA	160.840
Maximum local rod diameter (weld)	0.386 in	0.386 in
Bottom/top end plug diameter	0.381 in	0.381 in
Rod pitch	0.495 in	0.495 in
Cladding outer diameter	0.381 in	0.381 in
Cladding inner diameter	0.3440 in	0.3440 in
Plenum length	7.283 in	115.906 in
Internal pressurization	ambient	652.5 psi
Source activity at beginning of life	2×10^9 n/s	NA
Aluminum spacer diameter	0.323 in	NA
Lower alumina pellet stack length	19.553 in	NA
Upper alumina pellet stack length	126.890 in	NA
Source capsule diameter	0.338 in	NA
Source capsule length	1.535 in	NA
Sb-Be pellet mass	NA	0.45 lb_m
Sb-Be pellet diameter	NA	0.339 in
Sb-Be pellet length	NA	0.630 in

Figure 4.2-1—U.S. EPR Fuel Assembly

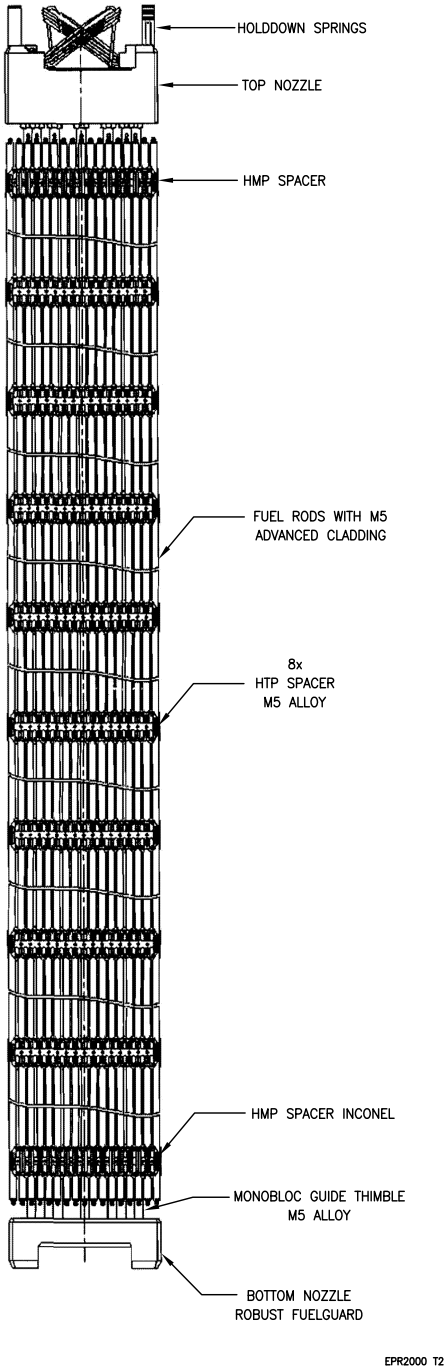

Figure 4.2-2—Fuel Rod Assembly

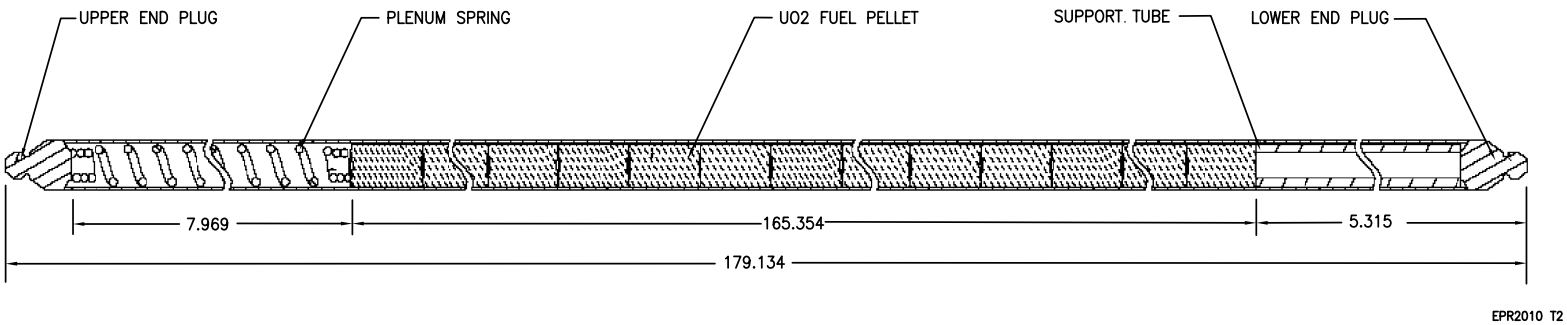

Figure 4.2-3—Instrument Lance Position

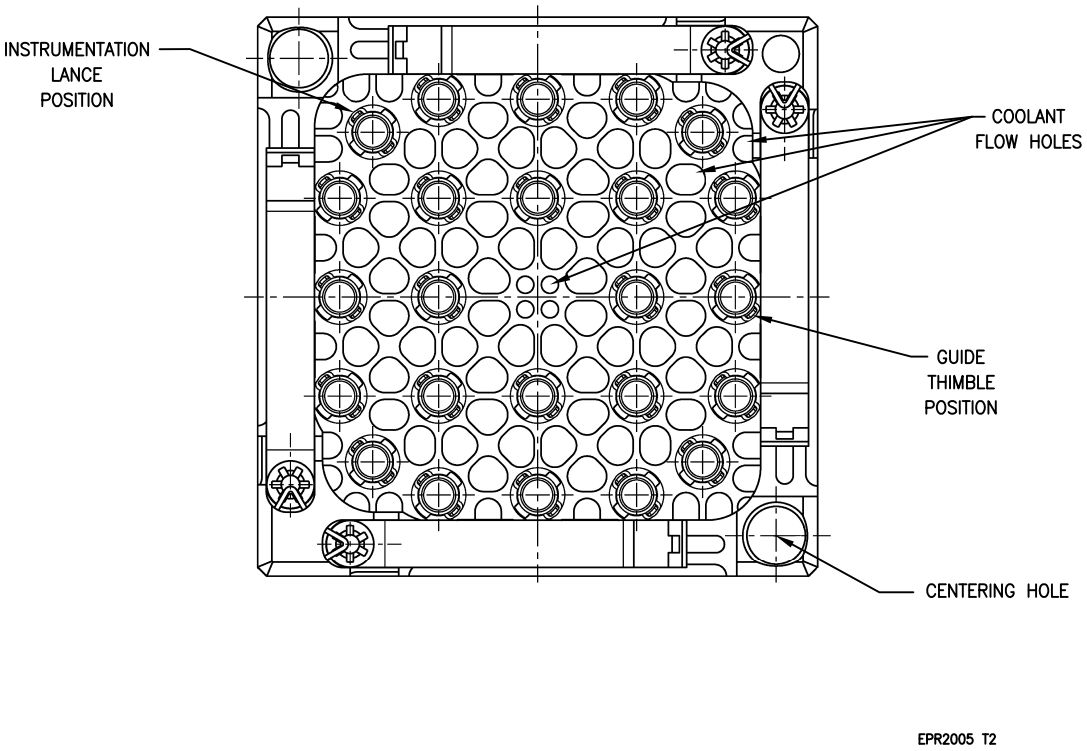

Figure 4.2-4—Intermediate HTP Spacer Grid Cross-Section

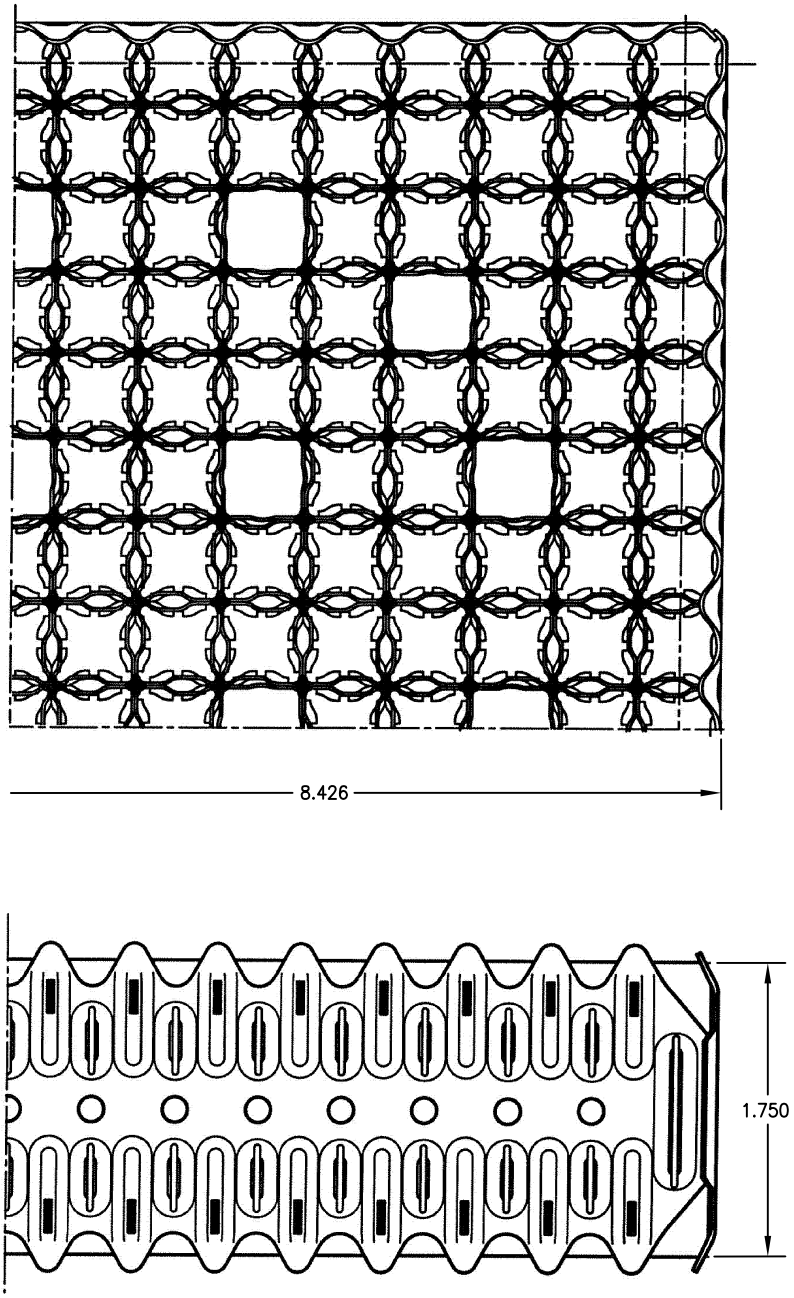

Figure 4.2-5—HTP Spacer Grid Characteristics

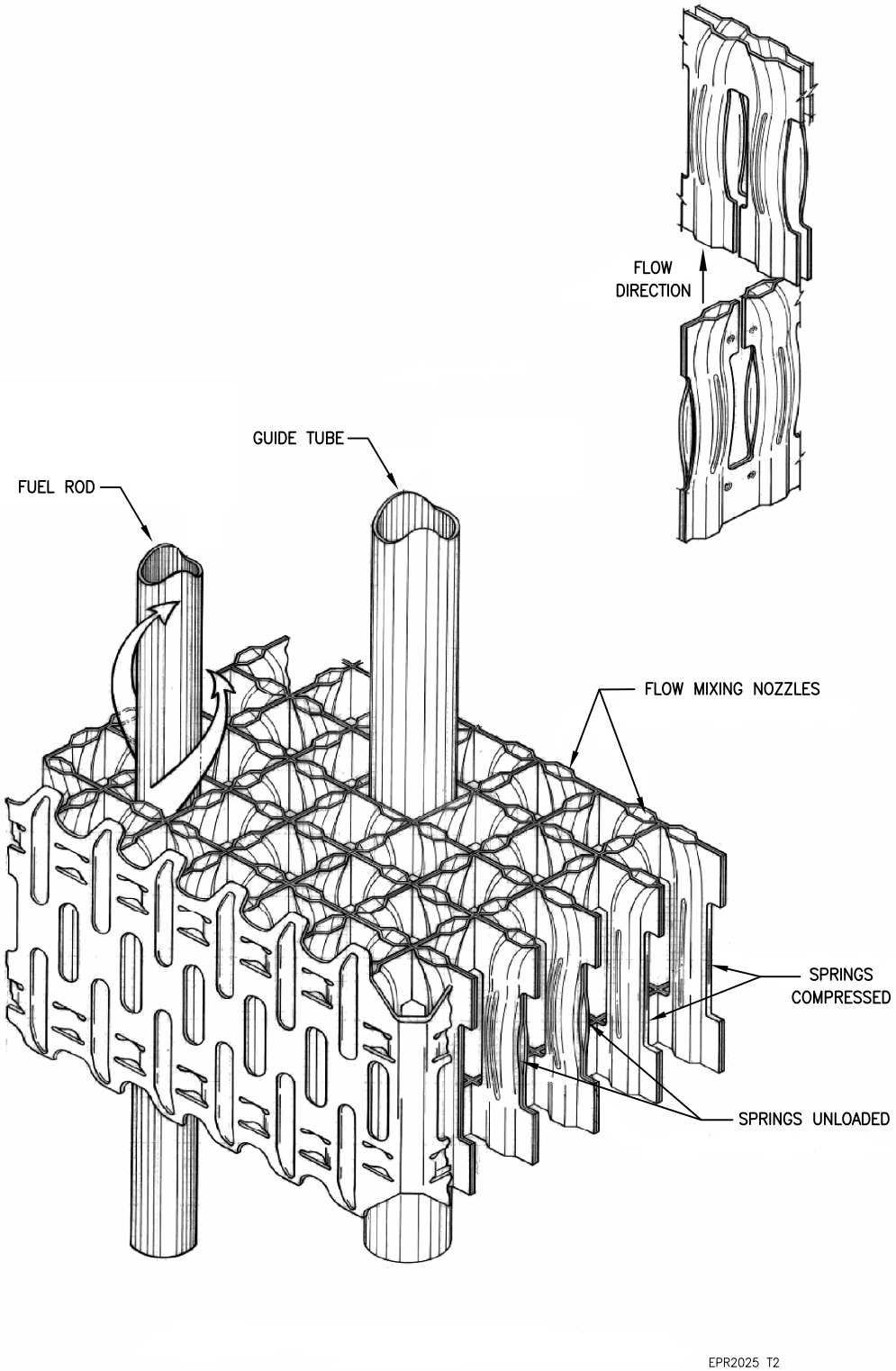

Figure 4.2-6—HMP End Grid Assembly

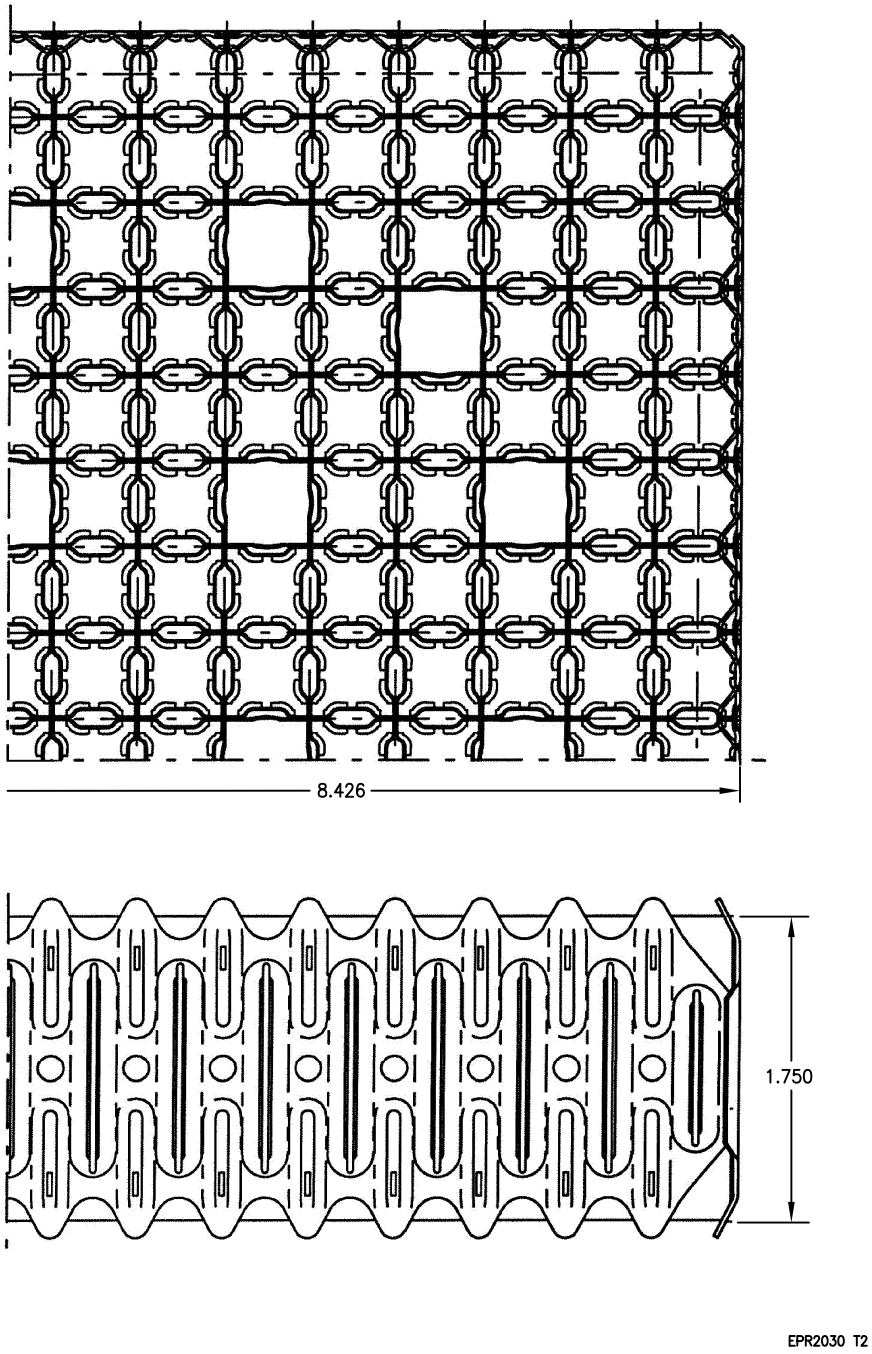

Figure 4.2-7—Guide Tube QD Connection with Top Nozzle

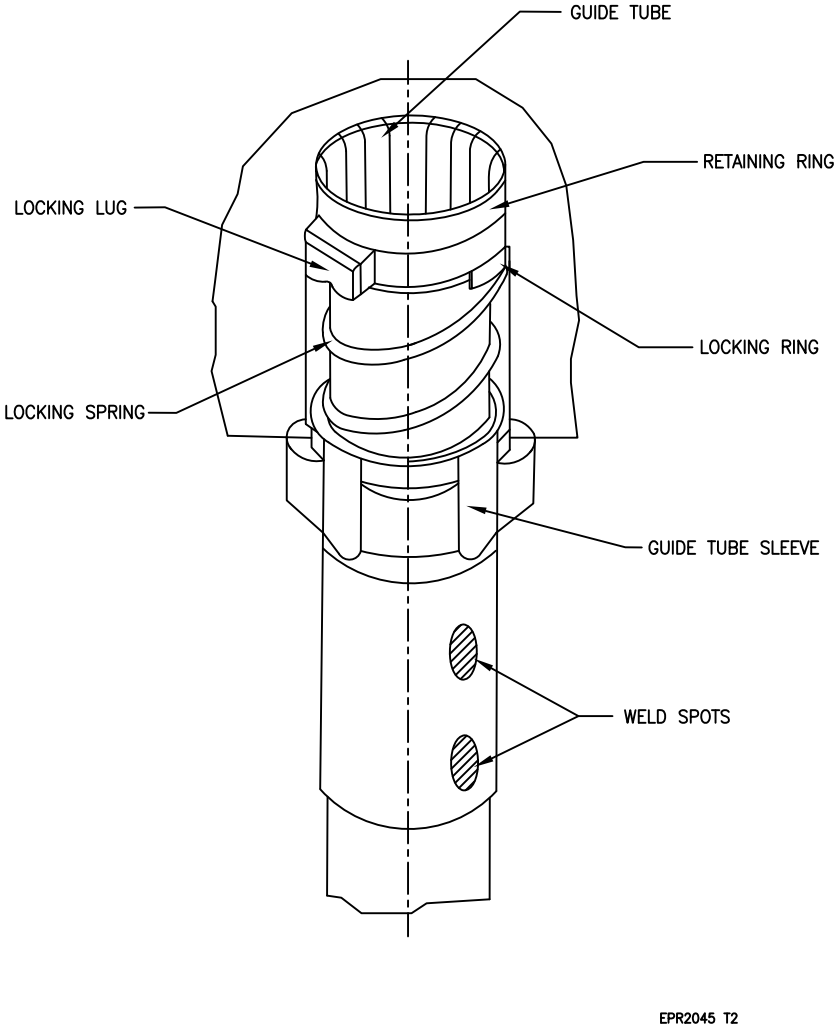

Figure 4.2-8—MONOBLOC™ Guide Tube Assembly

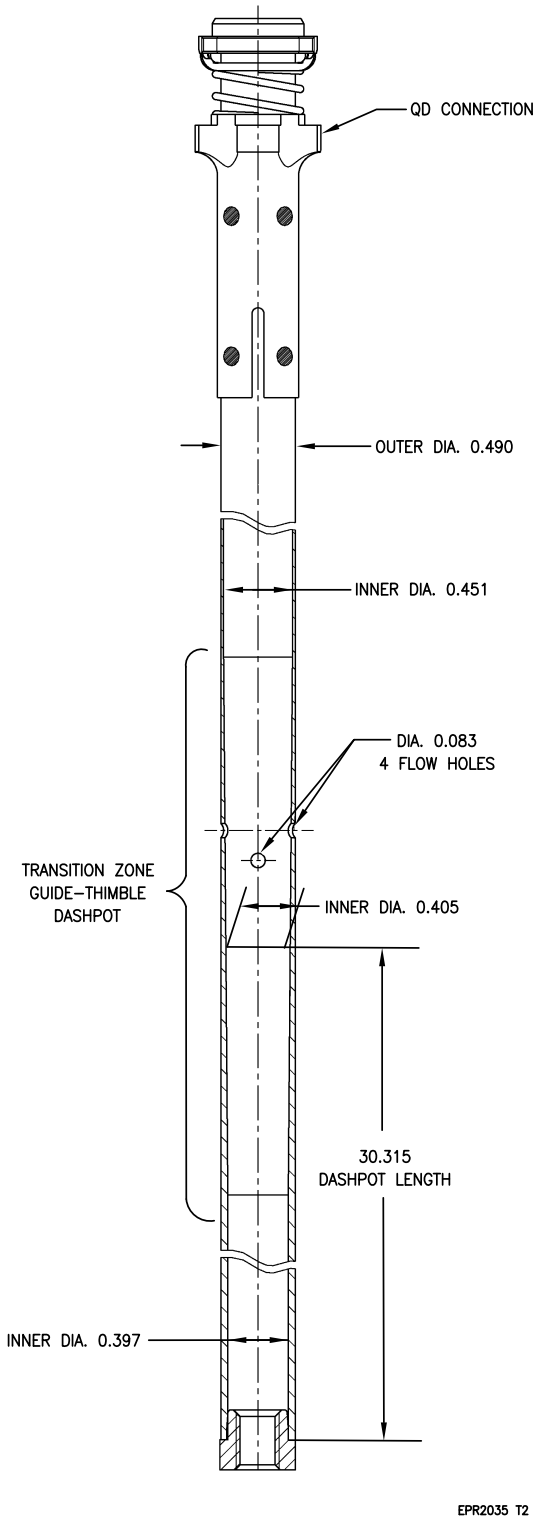

Figure 4.2-9—QD Top Nozzle Assembly

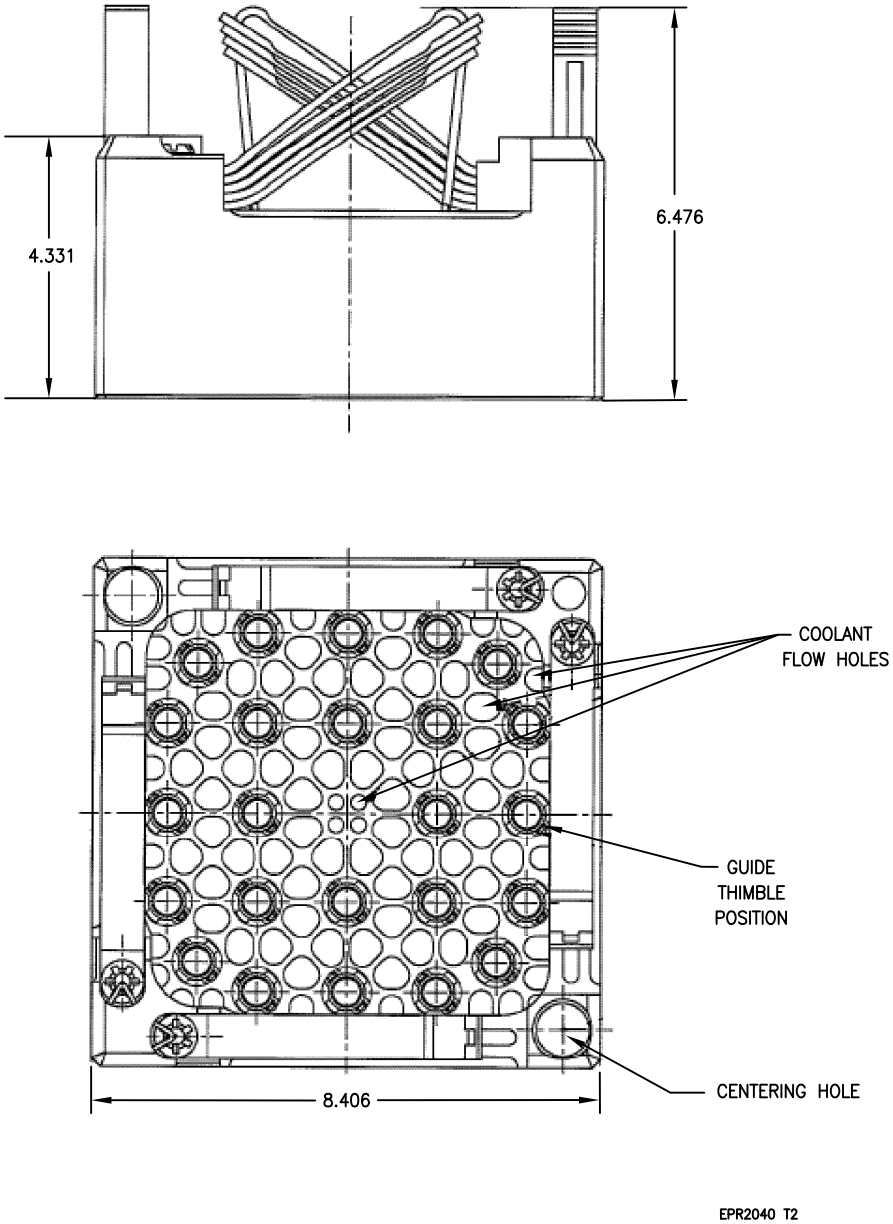

Figure 4.2-10—FUELGUARD™ Lower Nozzle Arrangement

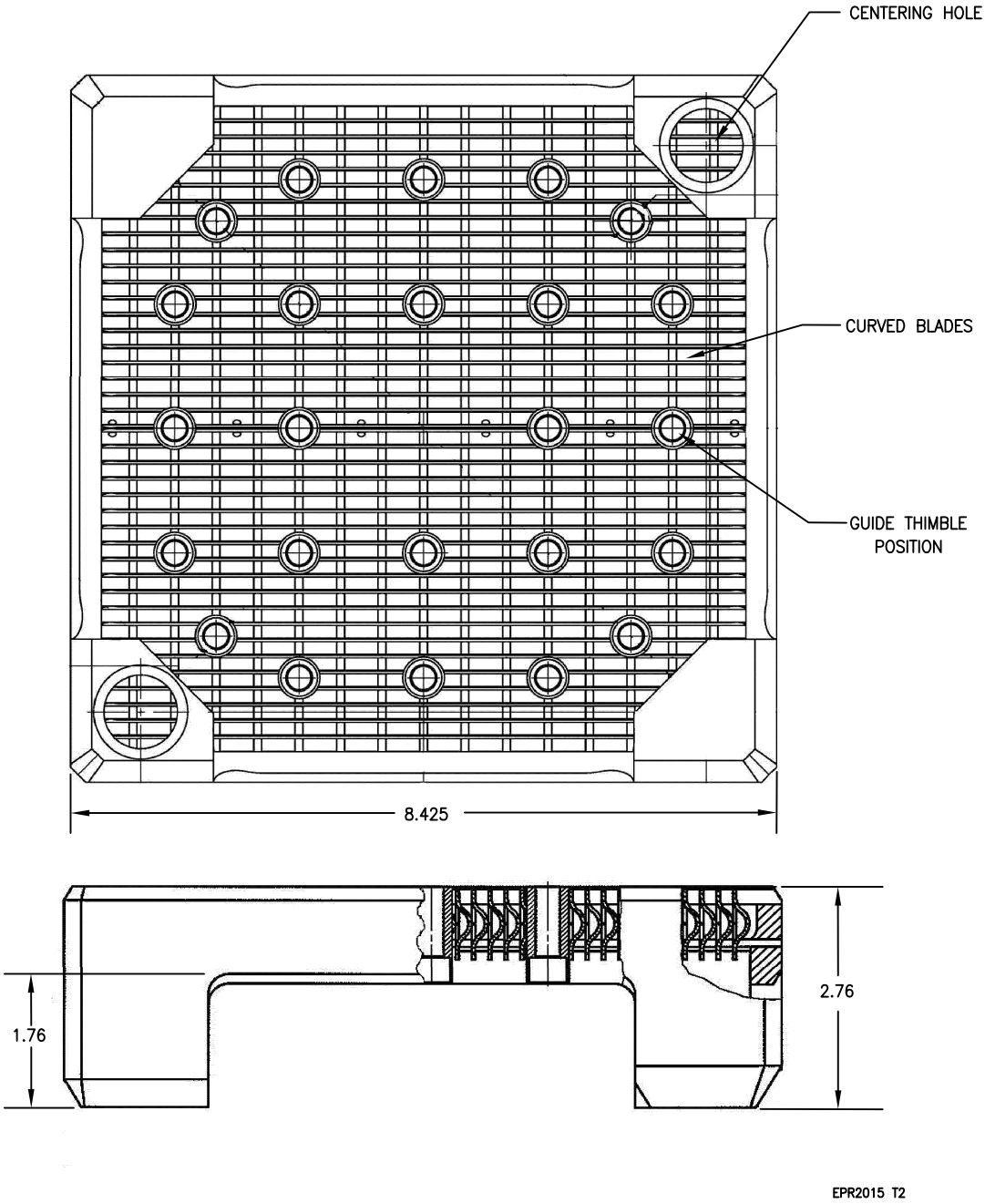

Figure 4.2-11—Guide Tube Screw Connection at Bottom Nozzle

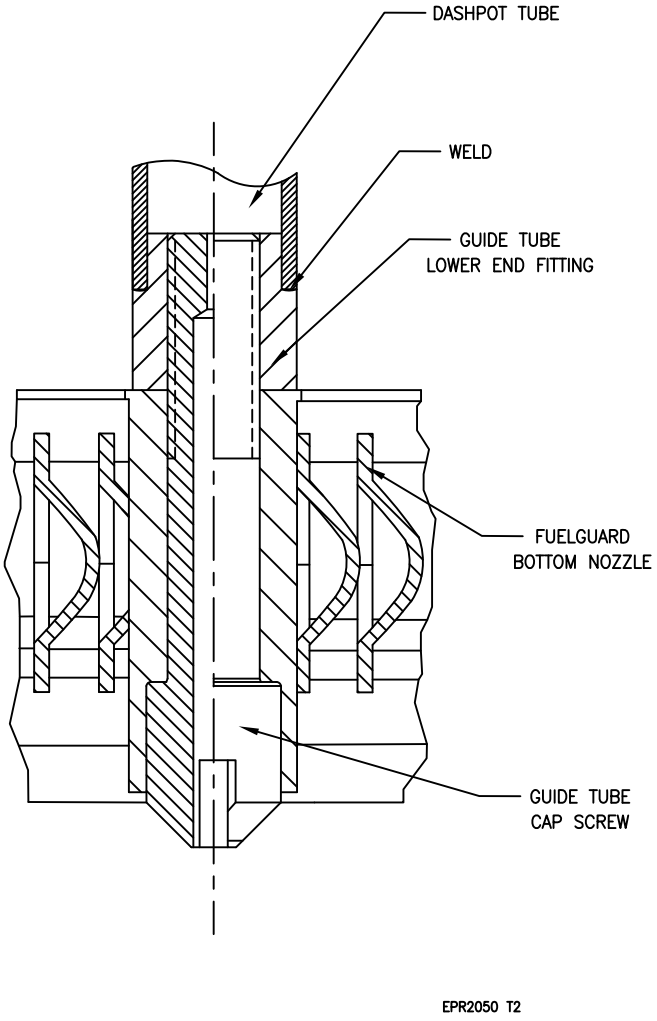

Figure 4.2-12—Rod Cluster Control Assembly

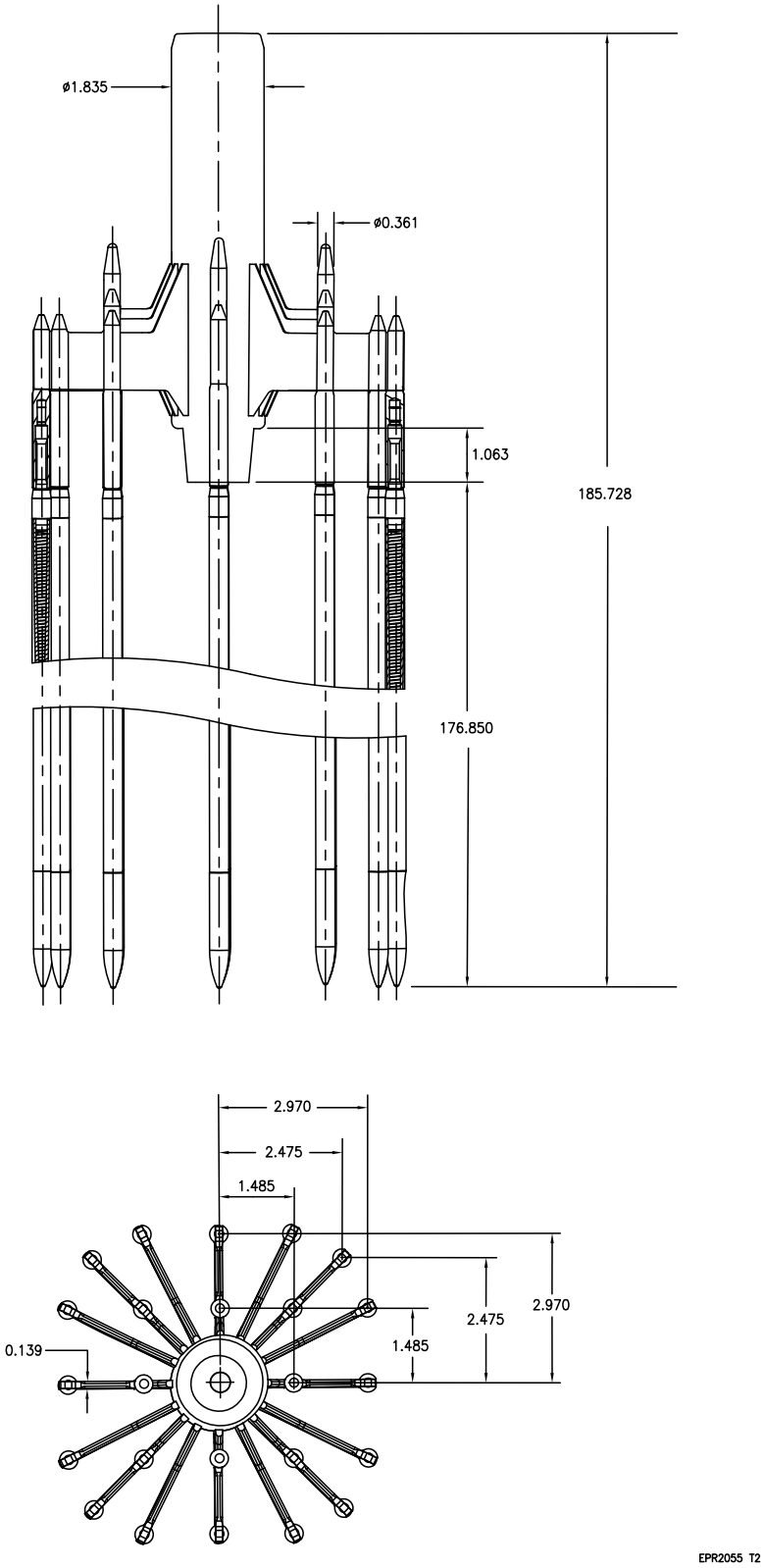

Figure 4.2-13—RCCA Control Rod

ITEM	DESCRIPTION
1	CONTROL ROD
2	UPPER END PLUG
3	PLENUM SPRING
4	ABSORBER
5	LOWER END PLUG

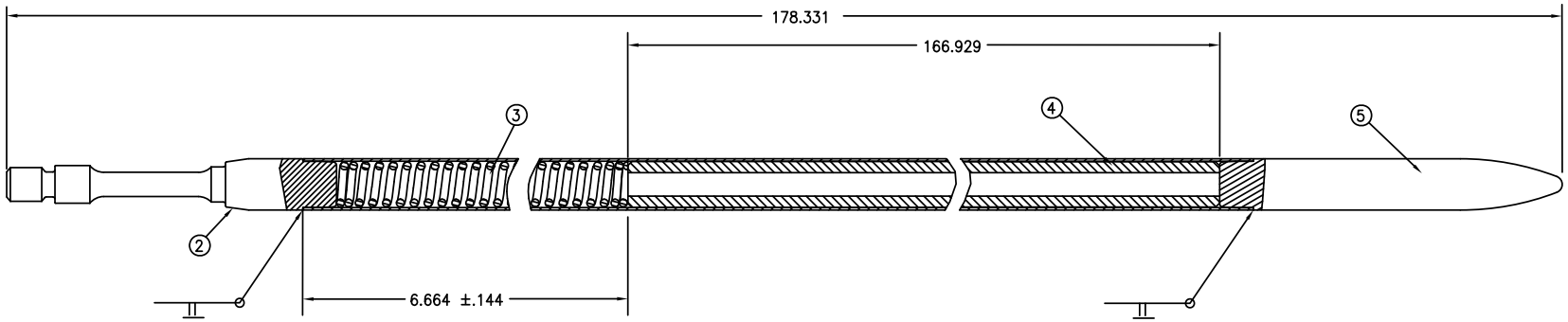

1 CONTROL ROD ASSEMBLY

EPR2060 T2

Figure 4.2-14—RCCA Spider

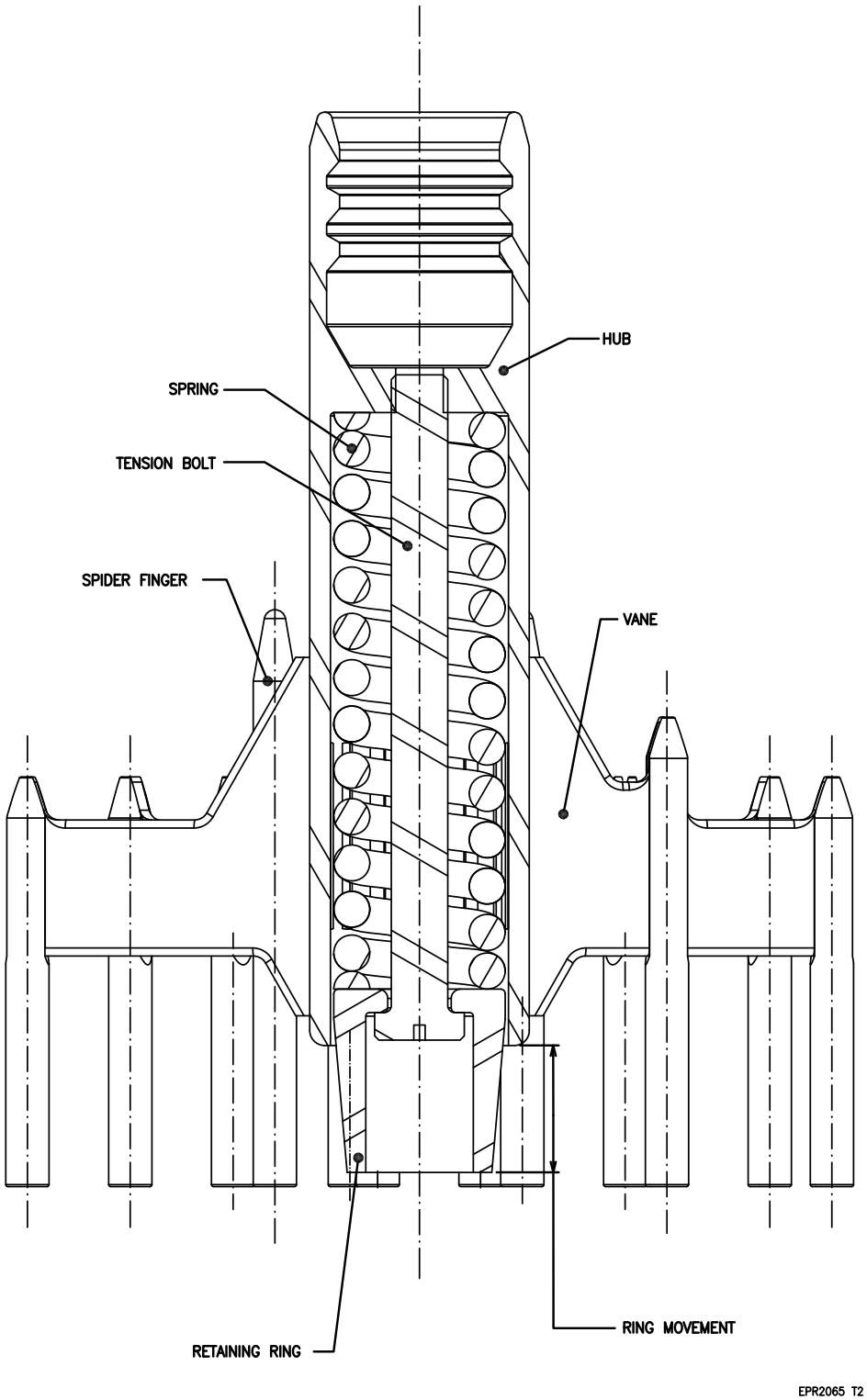

Figure 4.2-15—Thimble Plug Assembly

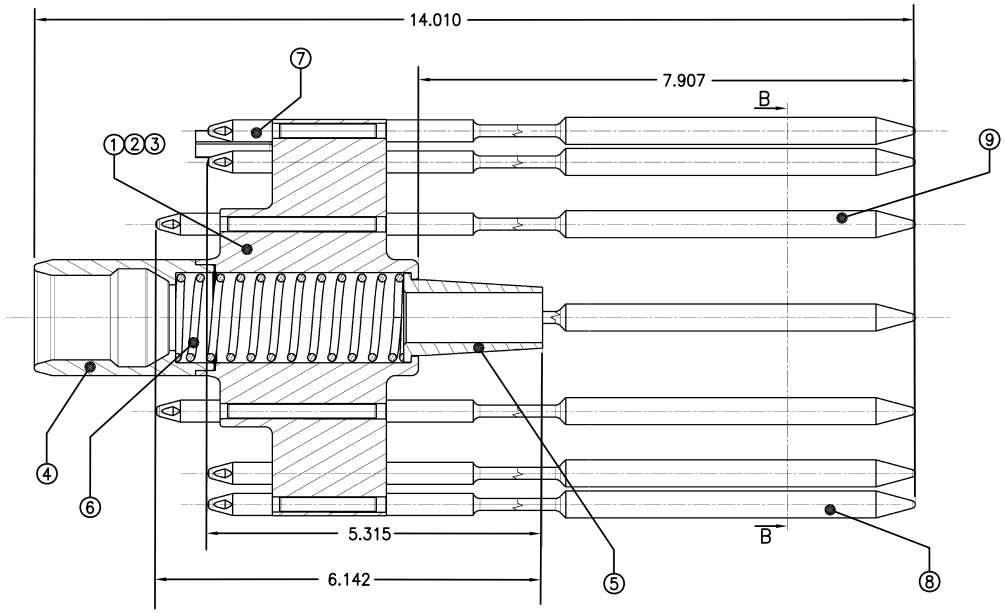

ITEM	PART DESCRIPTION	QTY
1	VANED HUB (0 RINGS)	1
2	VANED HUB (1 RINGS)	1
3	VANED HUB (2 RINGS)	1
4	COUPLING HUB	1
5	RETAINING RING	1
6	SPRING	1
7	BULLET HEAD NUT	24
8	THIMBLE PLUG – SHORT	20
9	THIMBLE PLUG – LONG	4

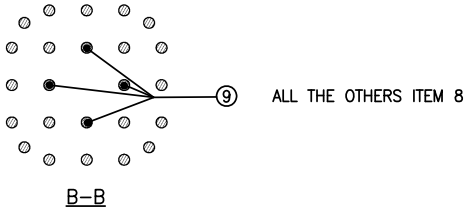

EPR2070 T2

Figure 4.2-16—TPA Spider Showing the Guide Ring Positions

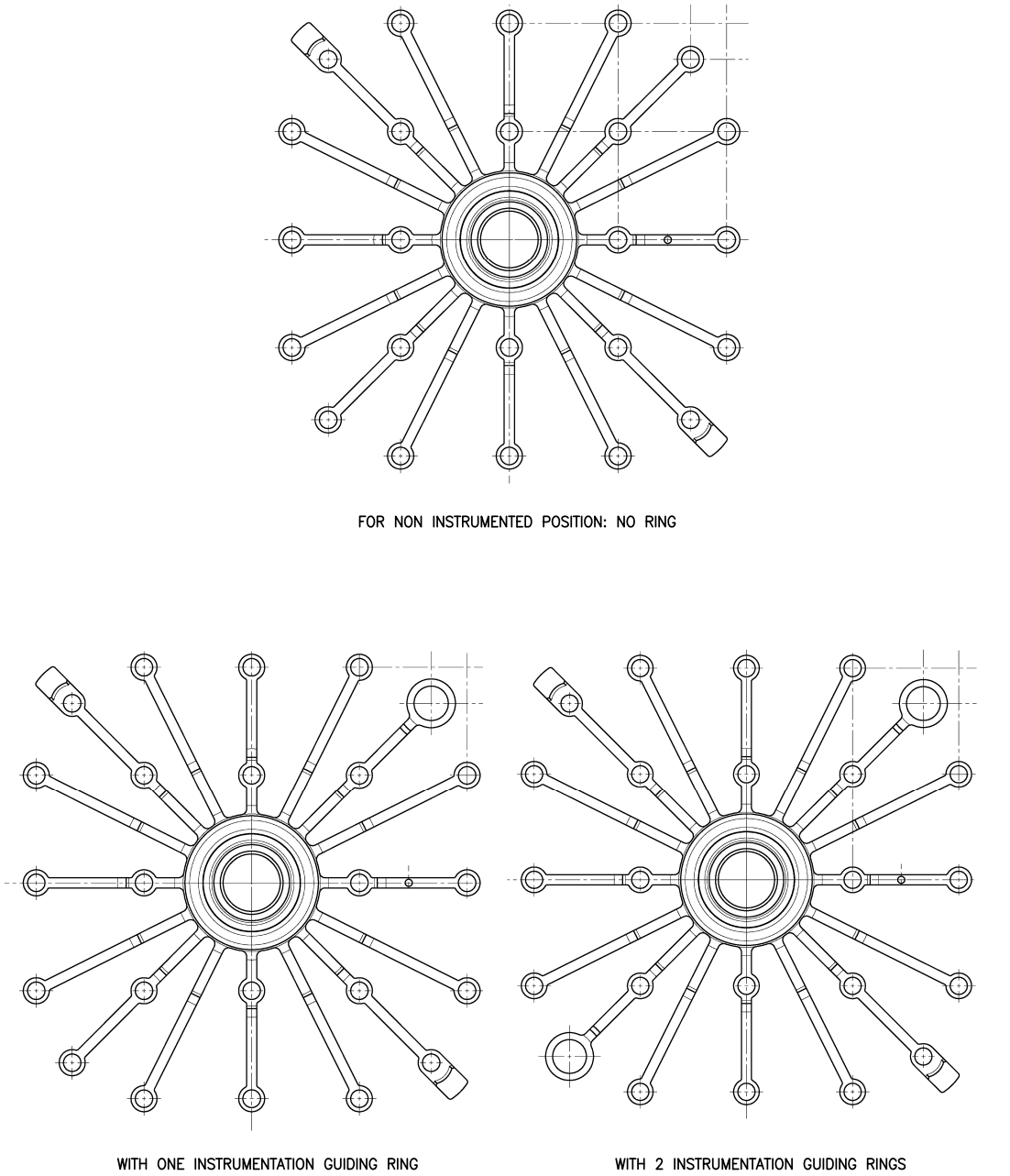

Figure 4.2-17—Primary Source Assembly

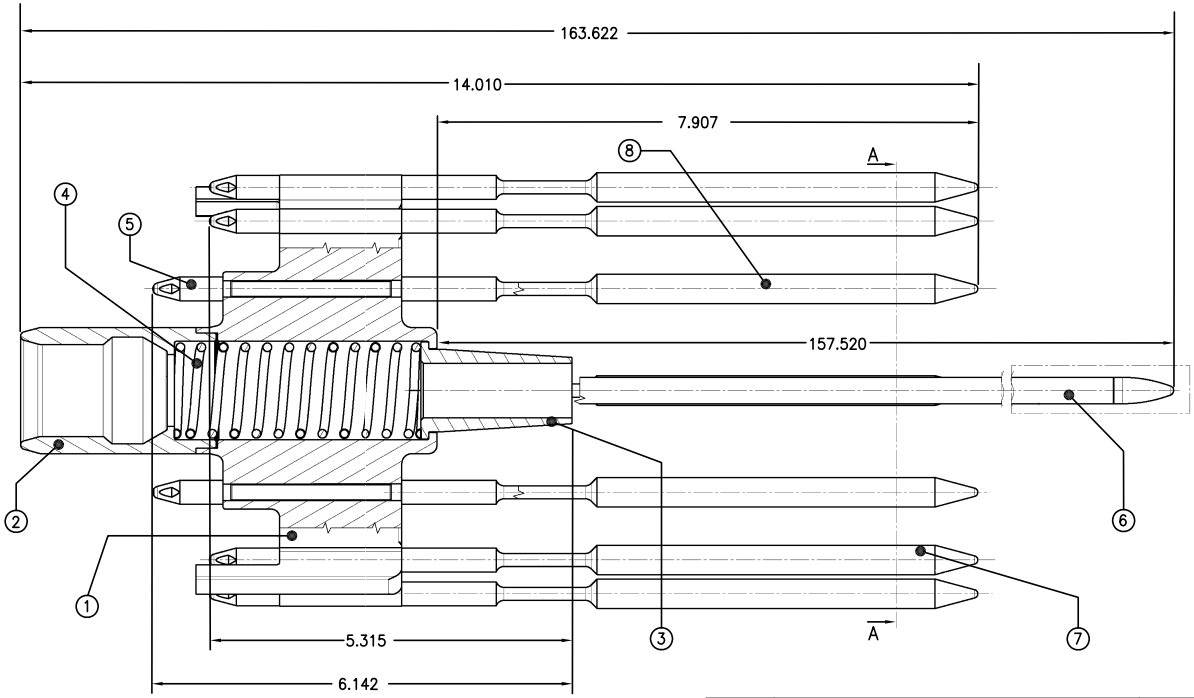

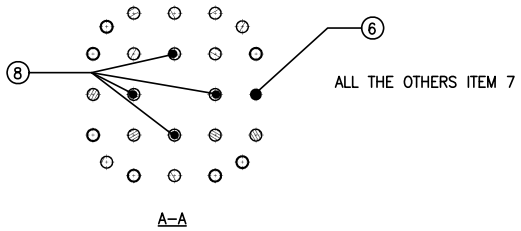

ITEM	PART DESCRIPTION	QTY
1	VANED HUB (0 RINGS)	1
2	COUPLING HUB	1
3	RETAINING RING	1
4	SPRING	1
5	BULLET HEAD NUT	24
6	PRIMARY SOURCE ROD	1
7	THIMBLE PLUG – SHORT	19
8	THIMBLE PLUG – LONG	4

EPR2085 T2

Figure 4.2-18—Secondary Source Assembly

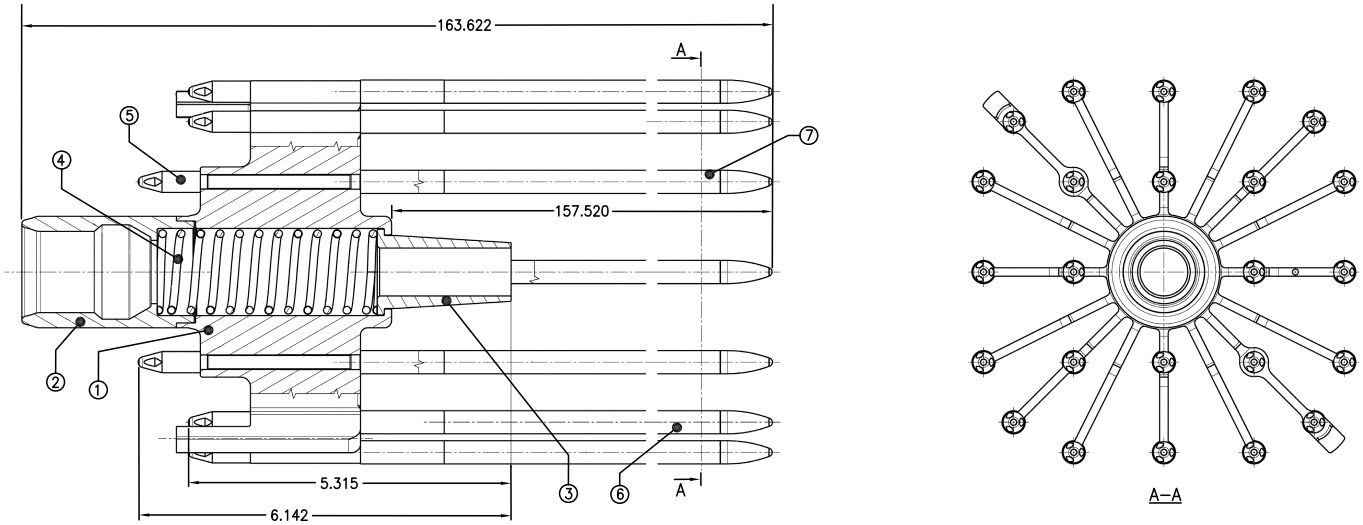

ITEM	PART DESCRIPTION	QTY
1	VANED HUB (0 RINGS)	1
2	COUPLING HUB	1
3	RETAINING RING	1
4	SPRING	1
5	BULLET HEAD NUT	24
6	SECONDARY SOURCE ROD – SHORT	20
7	SECONDARY SOURCE ROD – LONG	4

EPR2095 T2

Figure 4.2-19—Primary Neutron Source Rod

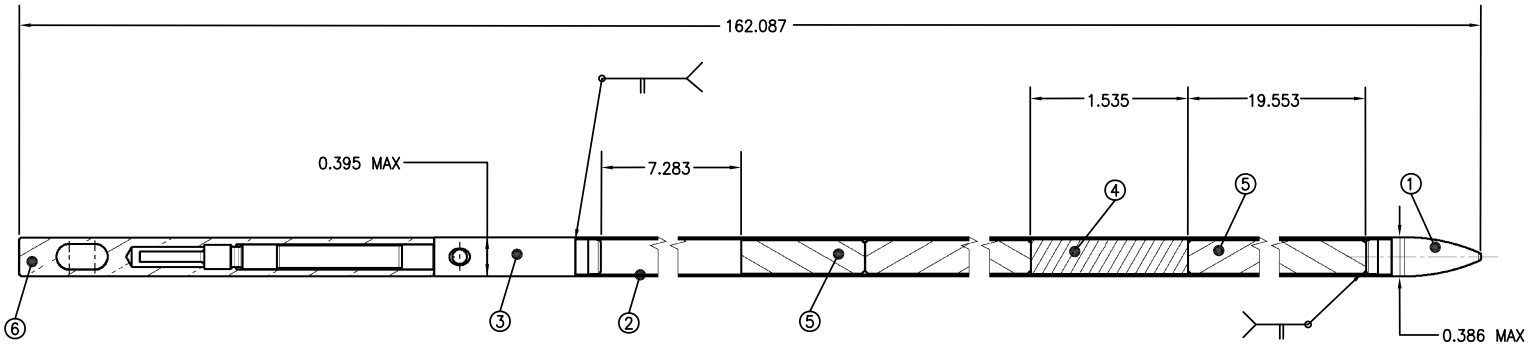

ITEM	ITEM DESCRIPTION	QTY
1	LOWER END PLUG	1
2	CLADDING TUBE	1
3	UPPER END PLUG	1
4	PRIMARY SOURCE CAPSULE	1
5	ALUMINA SPACER	~52
6	HANDLING ELEMENT	1

EPR2090 T2

Figure 4.2-20—Secondary Neutron Source Rod

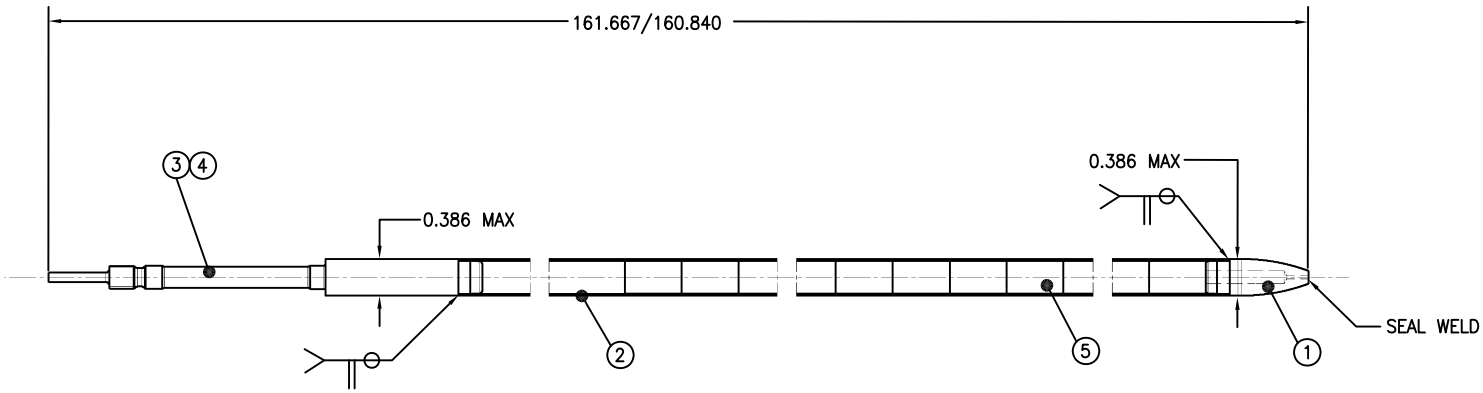

ITEM	PART DESCRIPTION	QTY
1	LOWER END PLUG	1
2	CLADDING TUBE	1
3	UPPER END PLUG (SHORT)	1
4	UPPER END PLUG (LONG)	1
5	Sb–Be PELLETS	~205 g

EPR2100 T2

Figure 4.2-21—Control Template

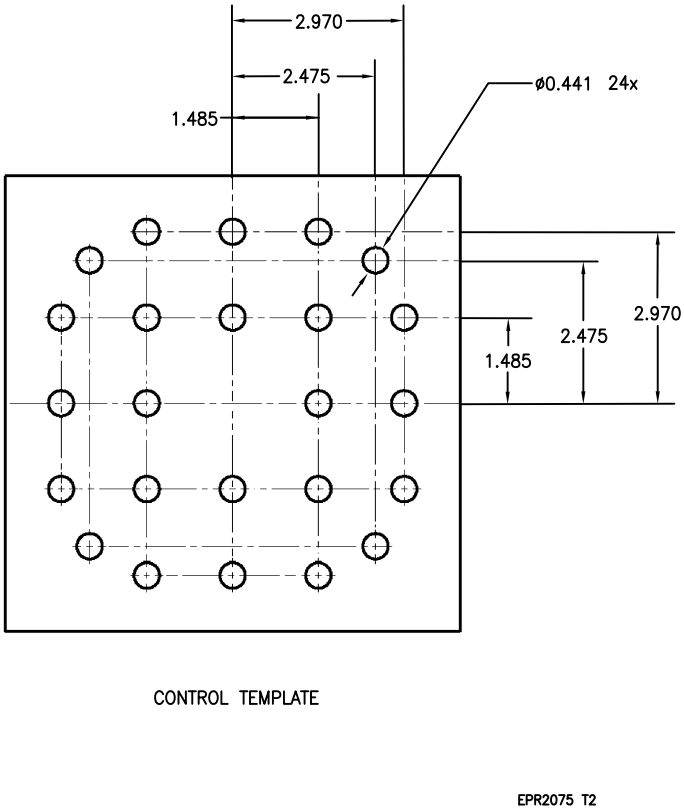

Next File